# NAVAL POSTGRADUATE SCHOOL
# MONTEREY, CALIFORNIA


# THESIS

**FIRE MODELING FOR COOK-OFF IN ORDNANCE MAGAZINES**

by

Timothy P. Callaham

December, 1996

Thesis Advisor: M. D. Kelleher

**Approved for public release; distribution is unlimited.**

# REPORT DOCUMENTATION PAGE

Form Approved OMB No. 0704-0188



| 1. AGENCY USE ONLY *(Leave blank)* | 2. REPORT DATE | 3. REPORT TYPE AND DATES COVERED |
|---|---|---|
| | **December 1996** | **Master's Thesis** |

4. TITLE AND SUBTITLE **FIRE MODELING FOR COOK-OFF IN ORDNANCE MAGAZINES**

5. FUNDING NUMBERS

6. AUTHOR(S) Callaham, Timothy P.

7. PERFORMING ORGANIZATION NAME(S) AND ADDRESS(ES)
Naval Postgraduate School
Monterey CA 93943-5000

8. PERFORMING ORGANIZATION REPORT NUMBER

9. SPONSORING/MONITORING AGENCY NAME(S) AND ADDRESS(ES)

10. SPONSORING/MONITORING AGENCY REPORT NUMBER

11. SUPPLEMENTARY NOTES The views expressed in this thesis are those of the author and do not reflect the official policy or position of the Department of Defense or the U.S. Government.

12a. DISTRIBUTION/AVAILABILITY STATEMENT
Approved for public release; distribution is unlimited.

12b. DISTRIBUTION CODE

13. ABSTRACT *(maximum 200 words)*

In this study, the time temperature profile of a missile exposed to fire in a compartment adjacent to the missile magazine is examined. The study required the development of a heat transfer model based on the geometry and thermophysical properties of a new concept for a vertical launching system, the Concentric Canister Launcher (CCL). Different fire scenarios are analyzed by the model to predict the time it takes to reach a critical value or "cook-off" temperature of the missile's propellant and explosives.

14. SUBJECT TERMS: Concentric Canister Launcher

15. NUMBER OF PAGES 117

16. PRICE CODE

| 17. SECURITY CLASSIFICATION OF REPORT | 18. SECURITY CLASSIFICATION OF THIS PAGE | 19. SECURITY CLASSIFICATION OF ABSTRACT | 20. LIMITATION OF ABSTRACT |
|---|---|---|---|
| Unclassified | Unclassified | Unclassified | UL |

NSN 7540-01-280-5500

Standard Form 298 (Rev. 2-89)
Prescribed by ANSI Std. 239-18 298-102

**Approved for public release; distribution is unlimited**

# FIRE MODELING FOR COOK-OFF IN ORDNANCE MAGAZINES

Timothy P. Callaham
Lieutenant, United States Navy
B.S., California Maritime Academy, 1989

Submitted in partial fulfillment of the
requirements for the degree of

**MASTER OF SCIENCE IN MECHANICAL ENGINEERING**

from the

**NAVAL POSTGRADUATE SCHOOL**
**December, 1996**

Author: _____
Timothy P. Callaham

Approved by: _____
Matthew D. Kelleher, Thesis Advisor

_____
Terry R. McNelley, Chairman
Department of Mechanical Engineering

# ABSTRACT

In this study, the time temperature profile of a missile exposed to fire in a compartment adjacent to the missile magazine is examined. The study required the development of a heat transfer model based on the geometry and thermophysical properties of a new concept for a vertical launching system, the Concentric Canister Launcher (CCL). Different fire scenarios are analyzed by the model to predict the time it takes to reach a critical value or "cook-off" temperature of the missile's propellant and explosives.

# TABLE OF CONTENTS

# LIST OF FIGURES

## LIST OF FIGURES (continued)

# LIST OF TABLES

# LIST OF SYMBOLS

$A$ = Area normal to heat transfer [$m^2$]
$c_{st}$ = Constant pressure specific heat of steel [J/(kg*K)]
$c_{ti}$ = Constant pressure specific heat of titanium [J/(kg*K)]
$d$ = Diameter [m]
$\dot{E}_{stored}$ = Rate of increase of stored energy within a solid [W]
$\dot{E}_{in}$ = Rate of energy transfer into a solid [W]
$F$ = View factor
$Fo$ = Fourier number
$g$ = Gravitational constant [$m/s^2$]
$Gr_L$ = Grashof number
$\overline{h}$ = Average convection heat transfer coefficient [$W/(m^2*K)$}
$k_{st}$ = Thermal conductivity of steel [M/(m*K)]
$k_{ti}$ = Thermal conductivity of titanium [M/(m*K)]
$k_{air}$ = Thermal conductivity of air [M/(m*K)]
$L_{can}$ = Length of canister [m]
$\overline{N_u}$ = Nusselt number
$p$ = Previous time
$p+1$ = New time
$Pr$ = Prandtl number
$Ra_L$ = Rayleigh number
$R1_{cond}$ = Thermal resistance of bulkhead [K/W]
$R2_{cond}$ = Thermal resistance of 1st cylinder wall [K/W]
$R3_{cond}$ = Thermal resistance of 2nd cylinder wall [K/W]
$R_{conv}$ = Thermal resistance for convection [K/W]
$R_{rad}$ = Thermal resistance for radiation [K/W]
$r_4$ = 1st cylinder outer radius [m]
$r_3$ = 1st cylinder inner radius [m]
$r_2$ = 2nd cylinder outer radius [m]
$r_1$ = 2nd cylinder inner radius [m]
$s$ = Distance between missile center lines [m]
$T_1$ = Outer surface temperature of bulkhead [K]

## LIST OF SYMBOLS (continued)

$T_2$ = Inner surface temperature of bulkhead [K]
$T_3$ = Outer surface temperature of 1st cylinder [K]
$T_4$ = Inner surface temperature of 1st cylinder [K]
$T_5$ = Outer surface temperature of 2nd cylinder [K]
$T_6$ = Inner surface temperature of 1st cylinder [K]
$T_7$ = Outer surface temperature of missile [K]
$T_8$ = Temperature center of missile [K]
$\Delta T_{av}$ = Change in average temperature [K]
$\Delta t$ = Time step [s]
$\Delta x$ = Bulkhead thickness [m]
$q$ = Heat transfer rate [W]
$q_{cond}$ = Heat transfer rate for conduction [W]
$q_o$ = Heat transfer rate between two surfaces [W]
$V$ = Volume [$m^3$]

$\alpha$ = Thermal diffusivity [$m^2/s$]
$\beta$ = Thermal expansion coefficient [$K^{-1}$]
$\varepsilon$ = Emissivity
$\nu$ = Kinematic viscosity [$m^2/s$]
$\rho_{st}$ = Density of steel [$kg/m^3$]
$\rho_{ti}$ = Density of titanium [$kg/m^3$]
$\sigma$ = Stefan-Boltzmann constant [$W/m^2*K^4$]

# ACKNOWLEDGMENT

I would like to acknowledge the support of NAVSEA Code 03R12, for providing the motivation behind this area of research. Additionally, I would like to express my sincere appreciation to those who kept me motivated through this thesis. Professor Kelleher, whose guidance has been absolutely indispensable over the past year. Professor Gopinath, who was always on hand to answer a quick question, and sparked my interest in heat transfer early in my studies. Most of all I would like to thank my parents, Captain and Mrs. Tom Callaham, and my fiancé, Argie Cominos, for being a continuous source of support and motivation.

# I. INTRODUCTION

## A. BACKGROUND

The history of naval combat has shown that there is a demonstrated need to understand how shipboard fires, and their containment, affect ship survivability. Credible fire threat models are particularly helpful in assessing the adequacy of fire protection systems, and in providing baseline data to make sound damage control decisions to combat conflagrations which may jeopardize munition magazines. Fires initiated by the penetration and detonation of Excocet missiles, and sustained with their unspent missile propellent, were experienced by the USS STARK (FFG 31) in the Arabian Gulf and British ships during the Falkland conflict. In all instances, ship's survivability was seriously jeopardized. In the Falklands, a British ship was abandoned and later lost. In each instance, munitions magazines were threatened by fire that spread into adjacent compartments. Drastic measures were required to cool the munitions, and prevent the detonation of high explosive material and the ignition of solid propellent. [Ref. 1]

## B. CCL CONCEPT

Naval Surface Warfare Center Dahlgren Division (NSWC) [Ref. 2] is currently examining a new concept for a future vertical launching system, the Concentric Canister Launcher (CCL). This new launcher will provide greater firepower, flexibility, and lower cost based on its modular design, than the current MK 41 VLS. The CCL was originally proposed to replace the MK 26 Guided Missile Launching System (GMLS) aboard CGN 36, DDG 993, CG 47-51, and non VLS, DD 963 classes to enhance capability with

increased magazine capacity. Additionally, the CCL would be adaptable to forward fit new ships such as future DDG-51's, SC-21, Arsenal and Swath hull designs.

A schematic of the CCL is given in Figure 1. It consists of two concentric cylinders joined by sets of dual longerons. One end is open and the other is sealed with a hemispherical cap. The annulus between the inner and outer cylinder provides gas management by ducting discharge exhaust combustion gases at launch. Each canister carries one missile and fits into a ship's weapon module. The weapons module consists of a test tube type rack in which each missile canister is held by a shock collar at the main deck. Schematics of the ship's weapon module and shock collar are given in Figures 2 and 3, respectively. The potential advantages of this concept over the current MK 41 are:

- Round pressure vessels and one shot design allow for the lightest possible configuration. This frees up ship's weight restrictions and allows for more missiles to be carried.

- Missiles fire vertically, horizontally, or at any angle in between. Thus, allowing CCL's to be outfitted in geometrically constraining spaces such as the narrow hull designs of the swath and surface-effects ships.

- A shock collar mitigates the underwater shock at the main deck rather than the inner bottom or platform level.

- A wide assortment of different weapons loadouts, such as ships self defense weapons (Seasparrow AAW missiles), electronic warfare devices (chaff and flares), torpedoes (MK 46 and 50), remote sensing devices (sonobuoys) in addition to the current capabilities of the MK 41 VLS (TLAM, SLAM, NATACMS, SM-2, etc.).

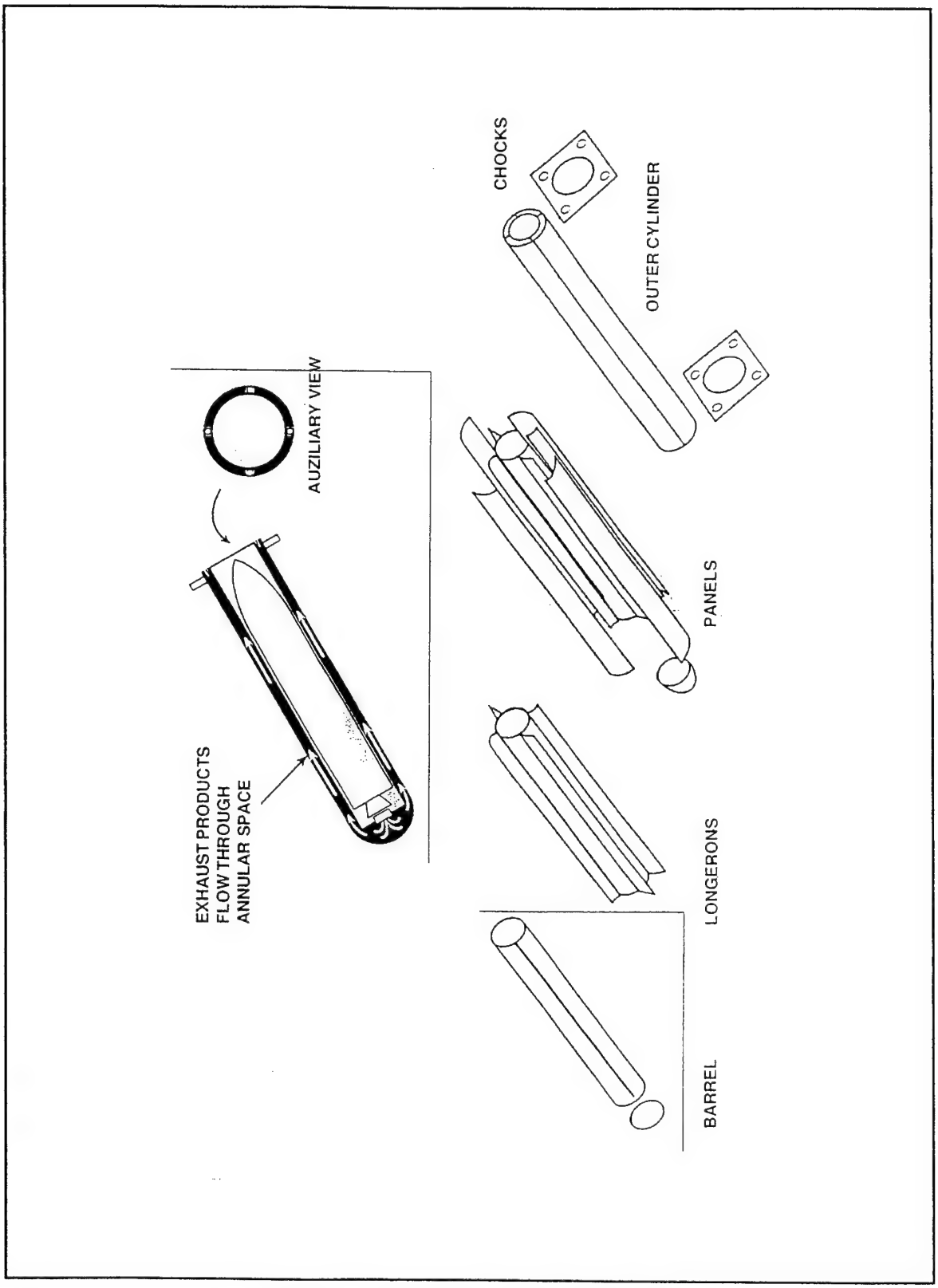


Figure 1. Concentric Canister Launcher.

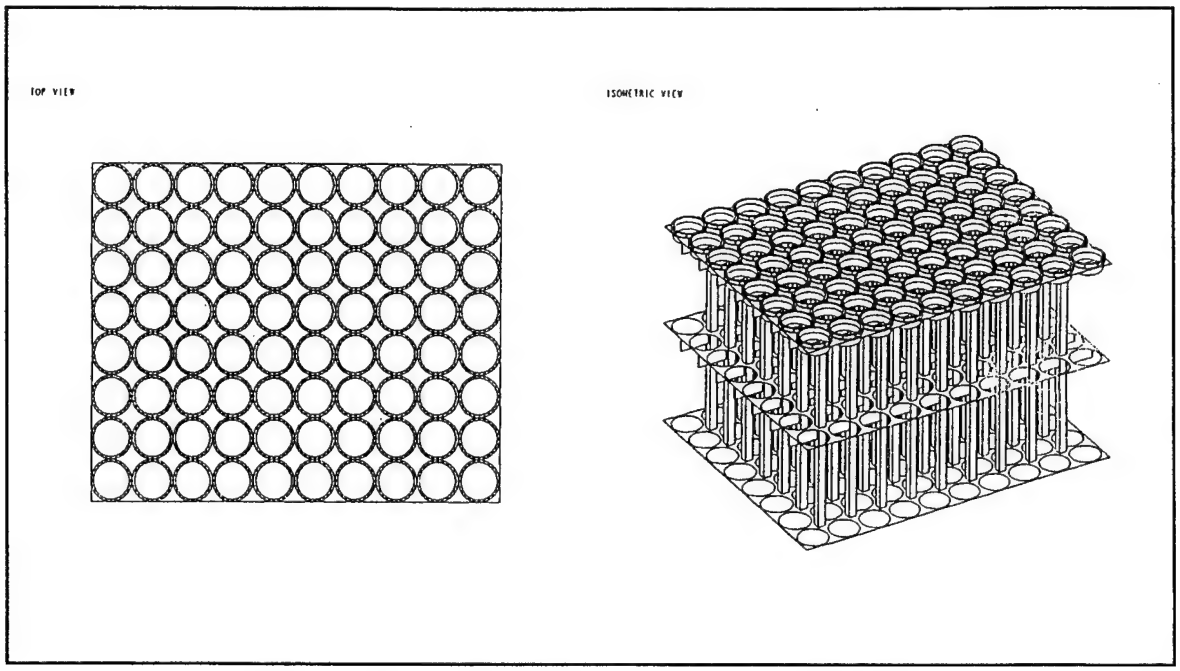


Figure 2. Ship's Weapons Module.

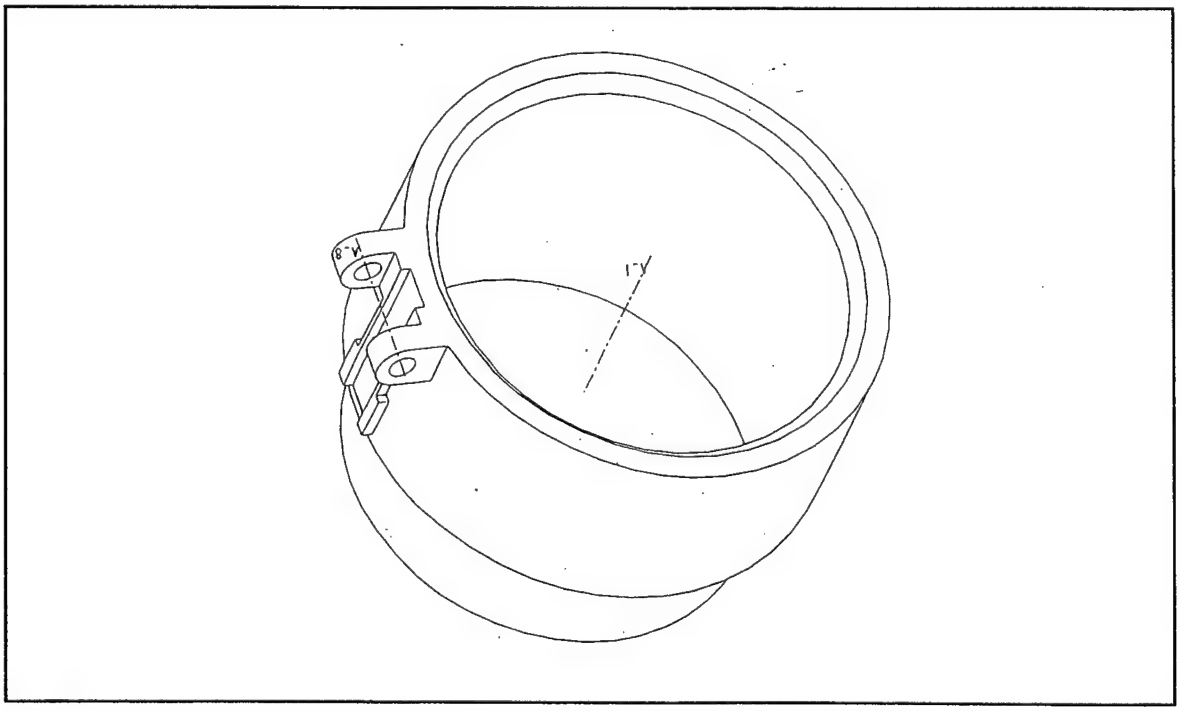

Figure 3. Shock Collar.

The CCL, although different from the MK 41 VLS, is not intended to replace it, but merely provides ship builders with a new set of options for launching a wide variety of weapons.

A CCL module sized to fit in the after VLS space of a DDG-51 ship contains up to 80 Tomahawk missiles. This weapons loadout contains approximately 24,000 lb. of solid propellant, 30,000 lb. of explosives, and 35,300 lb. of liquid fuel [Ref. 1]. Thus the fires experienced by British ships in the Falklands conflict and the USS STARK (FFG 31) involving this much high energy material has provided a vital insight into the dangers and difficulties of fire engulfing the spaces surrounding a CCL magazine. These incidents have aided greatly in the development of realistic scenarios to predict ship survivability.

## C. PREVIOUS WORK

Bowman and Lee [Ref. 1] developed a one dimensional heat transfer model to predict the time-temperature profiles in the missile canisters of the MK 41 VLS system for DDG-51 FLT I, II and IIA ships. Additionally, this model was used to evaluate the effectiveness of high temperature thermal insulation to reduce the heat transfer rates. Their scenarios used a fire in an adjacent compartment, which increased temperatures from ambient conditions to 2000°F in a period of five minutes, and then maintained that temperature for the duration of the fire.

Mansfield [Ref. 3] conducted an analysis of ordnance heating in steel walled compartments. He developed a computer algorithm that introduces heat into the fire compartment according to any selected fire size, and follows the heat transfer into the magazine and other compartments that surround the fire compartment. The output of this

algorithm is the calculation of the temperature of the fluid medium in the compartment and the surface temperature of the surrounding bulkheads, deck and overhead. It does not, however, take into account any varying geometry within the magazine.

## D. OBJECTIVES

The purpose of this study is to model a particular CCL within the module, specifically the CCL located in the first row along the centerline and corner, for a DDG-51 FLT-IIA ship. This one dimensional lumped parameter model describes the time-temperature profile in a Tomahawk missile to predict the time it takes to reach a critical value or "cook-off" temperature of propellant at the geometric center of the missile. Different fire intensities, temperatures and heat fluxes will be used to provide a wide baseline for comparison to real world scenarios.

# II. MODEL

## A. FORMULATION

The computer algorithm modeling the transfer of heat from a compartment on fire to a missile contained in a Concentric Canister Launcher (CCL) magazine is based on the electrical circuit analogy for heat transfer. Just as an electrical circuit is associated with the conduction of electricity, a thermal circuit may be associated with the transfer of heat [Ref. 4]. Therefore, the first step in the creation of the model is to develop a thermal network describing the heat transfer from the space to the missile taking into account the geometry of the CCL magazine. Time dependence is accounted for in the network by assigning a capacitance for the solid material of the bulkhead, canister walls, and missile. The input parameter to the algorithm is the rate of temperature increase on the outer surface of the bulkhead from ambient conditions to some specified steady value based on the fire scenario analyzed. Thermal conduction, convection and surface radiation are all accounted for in the model. Each one will be discussed along with the associated correlations, thermophysical properties, and geometry associated with its position in the thermal resistance network. The computer code for the heat transfer model is written in MATLAB 4.2.c. A schematic of the thermal resistance network is given in Figure 4.

### 1. Conduction

Conduction takes place in four locations in the resistance network. The first is the bulkhead which is modeled as a plane wall constructed of mild steel, AISI 1020. The thermophysical property data for this material were obtained from Touloukian's,

"Thermophysical Properties of Matter" [Ref. 6]. The data were curve fitted using MATLAB to form a polynomial to develop a smooth curve that "best fits" the property data and can be evaluated easily by the algorithm. The properties required for the algorithm are thermal conductivity ($k_{st}$), specific heat ($c_{st}$), and density ($\rho_{st}$). Each were evaluated at the average temperature between the two surfaces of the bulkhead. The thermal resistance for conduction through the bulkhead is given by the equation

$$RI_{cond} = \frac{\Delta x}{k_{st} A_1} \tag{1}$$

where ($\Delta x$) is the bulkhead thickness and ($A_1$) is the area normal to heat transfer. Therefore, the thermal energy transferred through the solid due to conduction is described by the relationship;

$$q_{cond} = \frac{T_1 - T_2}{RI_{cond}} \tag{2}$$

The capacitance assigned to the bulkhead to account for time dependence is expressed in the form of the rate of increase in stored energy,

$$\dot{E}_{stored} = \rho_{st} c_{st} V \left( \frac{\Delta T_{av}}{\Delta t} \right) \tag{3}$$

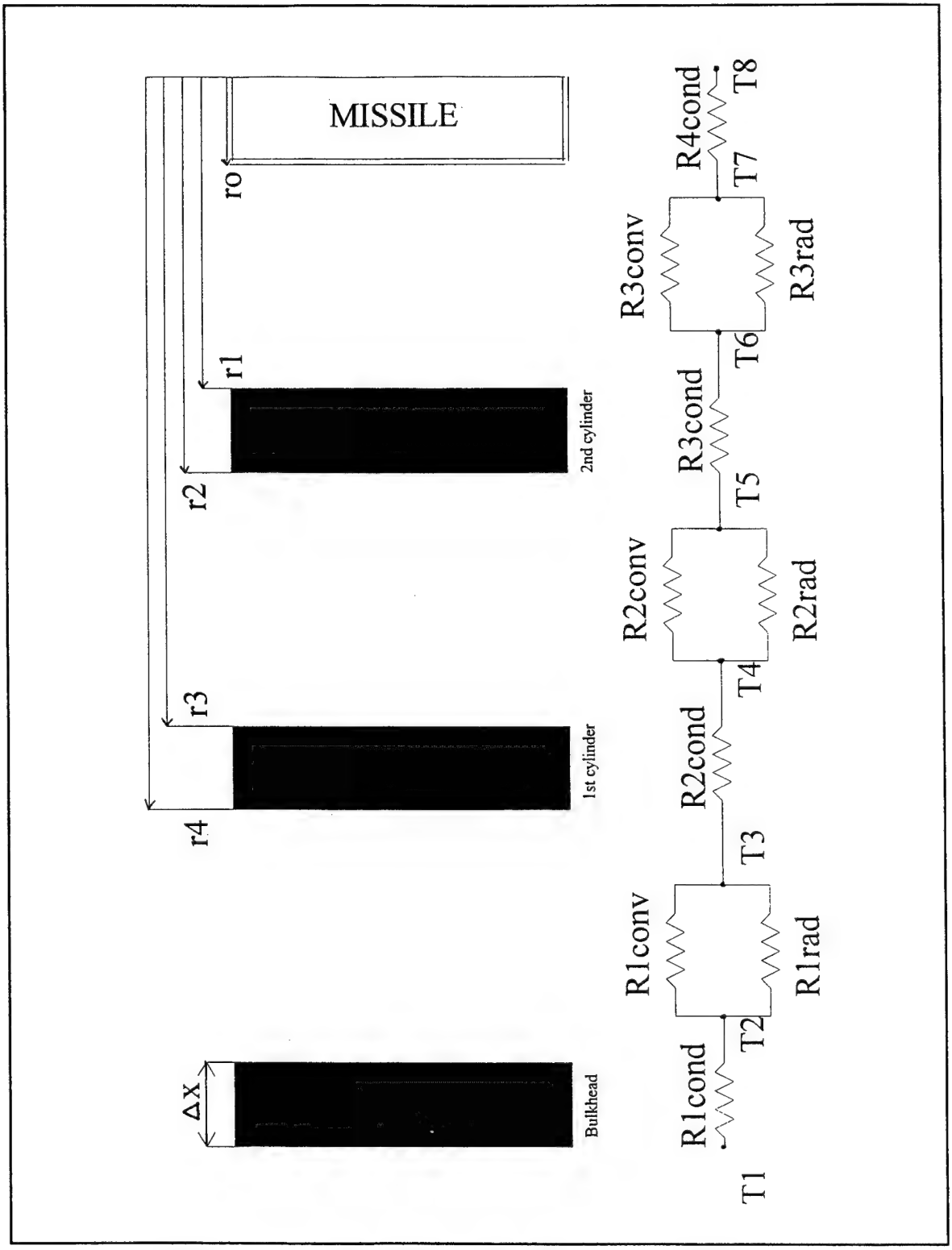


Figure 4. Thermal Resistance Network of the CCL Magazine.

where the average temperature is used to describe the temperature profile through the solid. This model assumes temperature profiles to be linear at any instant through solid material. The capacitance equation for stored energy remains the same for the cylinder walls and missile, except in the thermophysical properties associated with the different material used in their construction and in the calculation of the volume, which takes into account their different geometric shapes.

Conduction through the outer and inner cylinder walls is evaluated similar to the bulkhead, except that it is modeled in cylindrical coordinates and through walls constructed of titanium. Their thermophysical properties are again obtained from Touloukian, and are curve fitted with MATLAB to form a polynomial for use by the algorithm [Ref. 6]. The thermal resistance equations for conduction in the outer and inner cylinder wall are;

$$R2_{cond} = \frac{\ln \frac{r_4}{r_3}}{2\pi\ k_{ti}\ L_{can}} \tag{4}$$

$$R3_{cond} = \frac{\ln \frac{r_2}{r_1}}{2\pi\ k_{ti}\ L_{can}} \tag{5}$$

The missile's thermal resistance is constructed in the same manner as above except the missile thermophysical properties are assumed to be aluminum and uniform throughout.

## 2. Convection

Natural convection occurs in three areas in the resistance network. The first is the space between the bulkhead and the outer surface of the CCL. The second is the annulus between the inner and outer cylinders, which function as the gas management system during missile launch. The third is the space between the inner cylinder and the surface of the missile. The fluid medium of each area is assumed to be air and is evaluated at a mean boundary layer temperature, termed the film temperature. The properties required for computing the convective resistance are thermal conductivity ($k_{air}$), kinematic viscosity ($\nu$), volumetric thermal expansion coefficient ($\beta$), and Prandtl number (Pr). The thermal resistance for convection for each air space is given by the equation

$$R_{conv}=\frac{1}{\bar{h}\times A} \tag{6}$$

where the calculation of the average convection heat transfer coefficient ( $\bar{h}$ ) is based upon the Nusselt number ( $\overline{N_u}$ ), thermophysical properties of air, and either the height (L) of the CCL or the bulkhead.

$$\bar{h}=\frac{\overline{N_u}\times k_{air}}{L} \tag{7}$$

The thermophysical properties of air were curve fitted from tables in Reference 4 for use by the computer algorithm. The Nusselt number is a dimension less heat transfer coefficient and provides a measure of the convection heat transfer occurring at the surface. Empirical correlations for the Nusselt number have been developed based on the geometry of each enclosed air space.

The first air space Nusselt numbers are calculated with respect to the bulkhead and the CCL's free convection boundary layer. The bulkhead's Nusselt number is determined by using a correlation for a vertical plate developed by Churchill and Chu that may be applied over an entire range of Rayleigh numbers [Ref. 4].

$$\overline{N_u} = \left( 0.825 + \frac{0.387 Ra_L^{\frac{1}{6}}}{\left[ 1 + \left( \frac{0.492}{Pr} \right)^{\frac{9}{16}} \right]^{\frac{8}{27}}} \right)^2 \qquad \textbf{(8)}$$

The same equation may be applied to the outer surface of the CCL if the boundary layer thickness is much less than the diameter of the cylinder. To check for this condition the following criterion must be met [Ref. 4].

$$\frac{d}{L_{can}} \geq \frac{35}{Gr_L^{\left(\frac{1}{4}\right)}} \qquad \textbf{(9)}$$

If this inequality is not met, then curvature effects are appreciable and must be accounted for using the following correlation by Le Fevre and Ede [Ref. 5];

$$\overline{N_u}=\frac{4}{3}\left(\frac{7Gr_L\,Pr^2}{5(20+21Pr)}\right)^{\frac{1}{4}}+\frac{4(272+315Pr)L}{35(64+63Pr)d} \qquad \textbf{(10)}$$

The Grashof (Gr) and Rayleigh (Ra) numbers used throughout these correlations are given by:

$$Gr_L=\frac{g\beta(T_2-T_3)L^3}{\nu^2} \qquad \textbf{(11)}$$

$$Ra_L=Gr_LPr \qquad \textbf{(12)}$$

After each Nusselt correlation is computed, the average convective heat transfer coefficient is calculated from Equation 7. Assuming both surfaces act as external free convection flows, resistances are calculated with respect to the boundary layers along the bulkhead and CCL's surface using Equation 6. These resistances are added in series to form the total convective resistance between the bulkhead and the outer surface of the CCL. A schematic of the resistances is given in Figure 5.

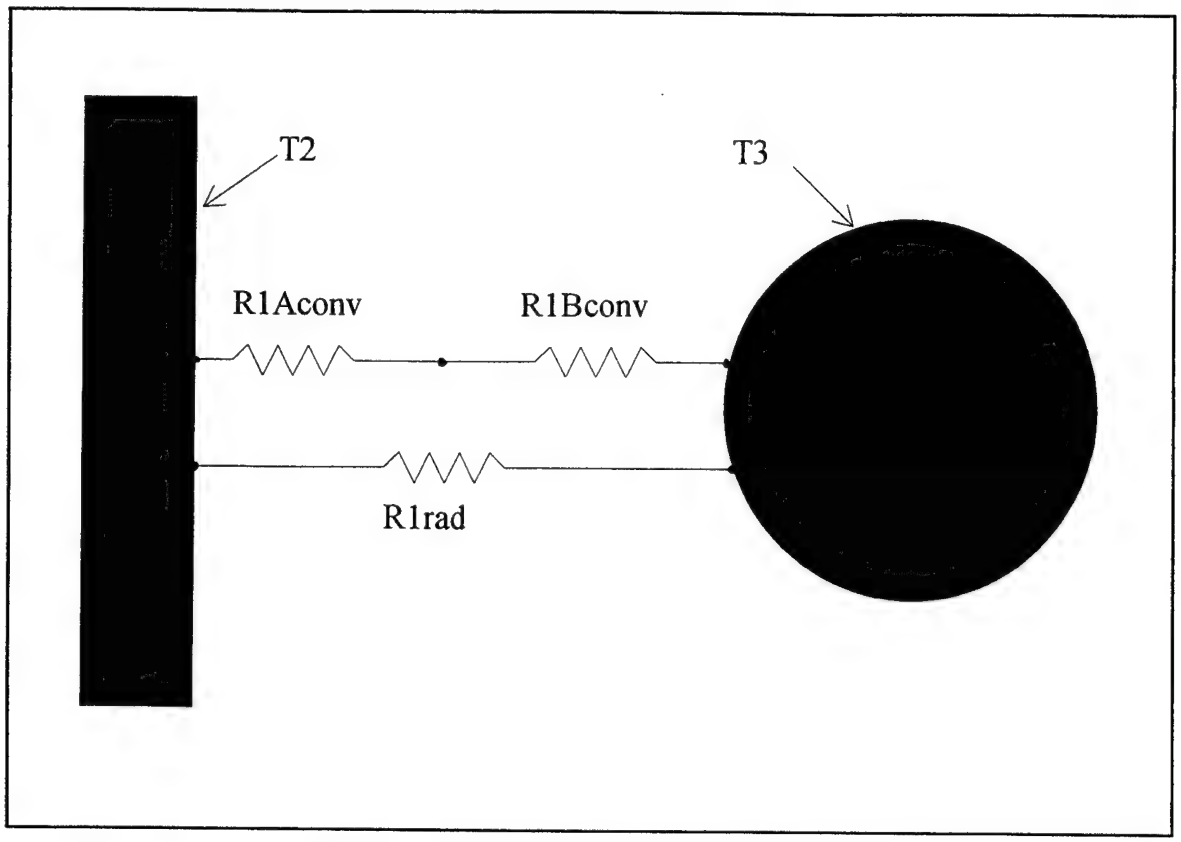


Figure 5. 1st Air Space Resistance Network.

The final two air spaces are circular annuli, and the Nusselt correlation used was developed by Churchill and Ozoe [Ref. 7].

$$\overline{N_u}=0.364\ (Ra_L\ f\ (Pr))^{\frac{1}{4}}\left(\frac{r_4}{r_3}\right)^{\frac{1}{2}} \tag{13}$$

where

$$f\ (Pr)=\left[1+\left(\frac{0.5}{Pr}\right)^{\frac{9}{16}}\right]^{\frac{-16}{9}} \tag{14}$$

In the two circular annuli only one resistance is calculated to describe the resistance across the enclosed space. The resistance and average convective heat transfer coefficient is again calculated using Equation 6 and 7, respectively. A schematic of the resistances across the annuli is given in Figure 6.

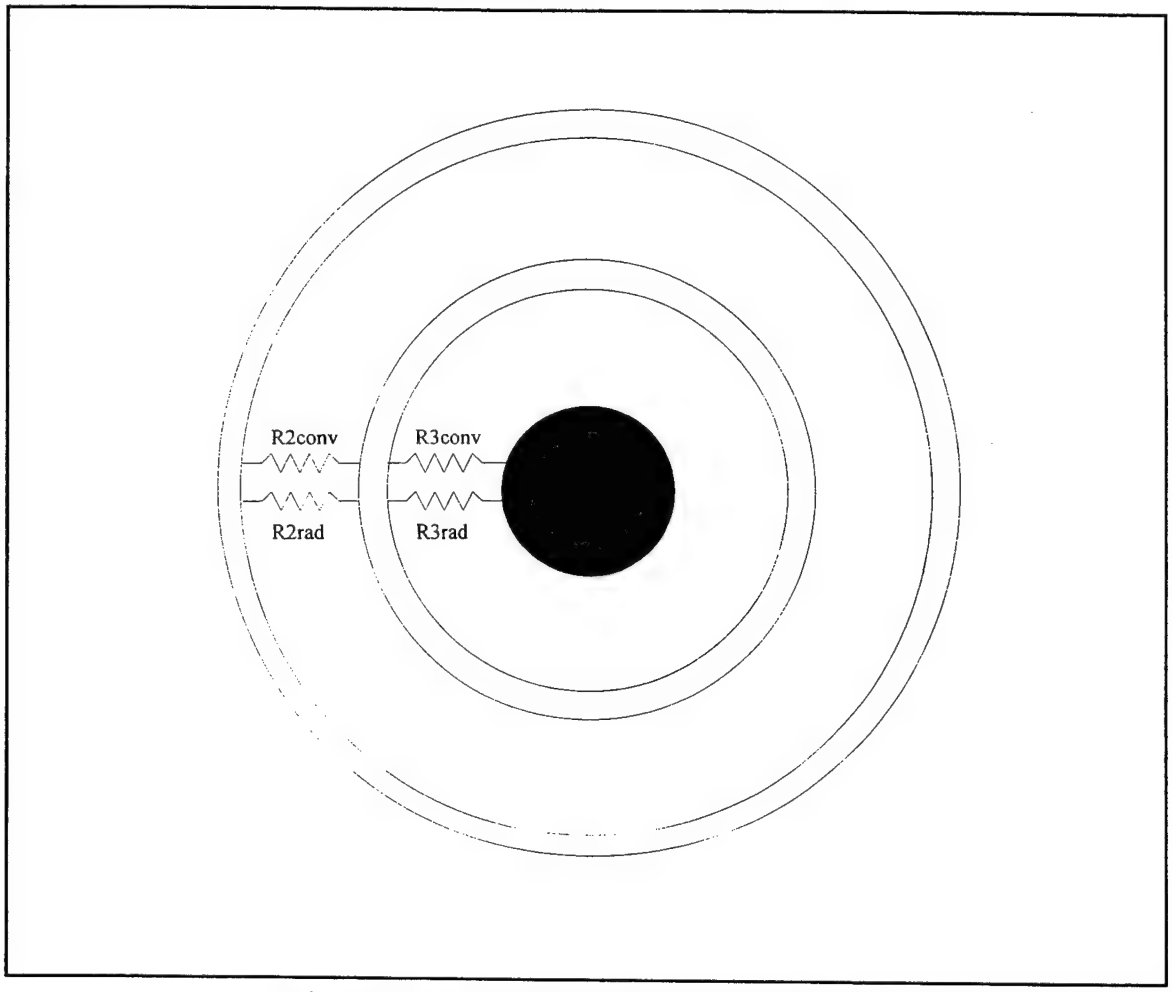


Figure 6. Resistance Network Across Annuli.

## 3. Radiation

Radiation affects heat transfer in the same air spaces as convection. Therefore, the thermal resistance for radiation and convection act in parallel, and can be combined to obtain a single effective surface resistance [Ref.4].

$$R_t = \frac{R_{conv}\, R_{rad}}{R_{conv} + R_{rad}} \tag{15}$$

The total resistance to radiation exchange between the surfaces is comprised of the two surface resistances and the geometrical resistance.

$$Rr_{tot} = \frac{1-\varepsilon_2}{\varepsilon_2 A_2} + \frac{1}{F_{23} A_2} + \frac{1-\varepsilon_3}{\varepsilon_3 A_3} \tag{16}$$

The radiative property used in the resistance calculations is emissivity (ε). The emissivity of the different materials is obtained from Touloukian [Ref. 6], and curve fitted to form a polynomial for use in the computer algorithm. The view factor ($F_{23}$) is explained later. Therefore, the net radiation exchange between surfaces is expressed as;

$$q_o = \frac{\sigma(T_2^4 - T_3^4)}{Rr_{tot}} \tag{17}$$

However, this equation is non-linear to the fourth power, and the overall radiative resistance ($R_{rad}$) must be solved, so the heat rate due to radiation takes the form;

$$q_{rad} = \frac{(T_2 - T_3)}{R_{rad}} \tag{18}$$

and can be used in conjunction with the convective resistance. This is accomplished using two different methods. The first is to linearize the equation by expanding in a Taylor series, and the second is to solve it explicitly. Using a Taylor series expansion on Equation 17 takes the form;

$$q_{rad}=q_o+\left(\frac{dq}{dT}\right)_{T=T_3}(T-T_3)+O[(T-T_3)^2] \tag{19}$$

and after linearizing, the resistance due to radiation becomes

$$\frac{1}{R_{rad}}=\frac{q_o}{(T_2-T_3)}+\frac{4\sigma T_3^3}{Rr_{tot}} \tag{20}$$

To solve for the overall radiative resistance explicitly, Equations 17 and 18 are set equal to each other and solved algebraically. The overall resistance due to radiation is then expressed as:

$$\frac{1}{R_{rad}}=\frac{\sigma}{Rr_{tot}}\left[(T_2+T_3)(T_2^2+T_3^2)\right] \tag{21}$$

Note that the resistance is temperature dependent. These two processes are used for all radiative resistances in the thermal resistance network, and will be compared in the final results. The difference in the geometric shapes of the enclosures are taken into account by

calculating the fraction of the radiation leaving one surface and intercepted by another. This is termed the view factor ($F_{23}$). In the first air space, the view factor is calculated as an infinite plane to a row of cylinders [Ref. 9].

$$F_{23}=1-(1-D^2)^{\frac{1}{2}}+D\ \arctan\left(\frac{1-D^2}{D^2}\right)^{\frac{1}{2}} \tag{22}$$

where

$$D=\frac{d}{s} \tag{23}$$

In the final two air spaces, the view factors are calculated as the interior of an outer right circular cylinder of finite length to the exterior of a inner right circular coaxial cylinder of finite length [Ref. 10].

$$F_{45}=\frac{1}{R}\left(1-\frac{H^2+R^2-1}{4H}-\frac{1}{\pi}\left[\cos^{-1}\frac{H^2-R^2+1}{H^2+R^2-1}-\frac{\sqrt{(H^2+R^2+1)^2-2R^2}}{2H}\times\right.\right.$$

$$\left.\left.\cos^{-1}\ \frac{H^2-R^2+1}{R(H^2+R^2-1)}-\frac{H^2-R^2+1}{2H}\ \sin^{-1}\ \frac{1}{R}\right]\right) \tag{24}$$

where

$$H=\frac{L_{can}}{r_2} \tag{25}$$

$$R=\frac{r_3}{r_2} \tag{26}$$

The thermal energy transferred through the air space is described by the relationship

$$q=\frac{T_2-T_3}{R_t} \tag{27}$$

where ($R_t$) is the total resistance due to radiation and convection, Equation 15.

The radiative resistance network thus far models a CCL on the first row near the centerline of the ship. As mentioned in the objectives, the CCL in the corner of the magazine is also modeled, accounting for the radiation effects of the adjoining bulkhead. The adjoining bulkhead is modeled as a reradiating surface. Equation 16 is modified to account for the radiation leaving the effected bulkhead, reflected off the adjoining bulkhead and absorbed by the surface of the CCL, and takes the form;

$$Rr_{tot}=\frac{1-\varepsilon_2}{\varepsilon_2 A_2}+\frac{1}{F_{23}A_2+\left[\frac{1}{F_{2R}A_2}+\frac{1}{F_{R3}A_R}\right]^{-1}}+\frac{1-\varepsilon_3}{\varepsilon_3 A_3} \tag{28}$$

The view factor from the reradiating bulkhead to the canister ($F_{R3}$) is the same as the view factor from the effected bulkhead to the canister ($F_{23}$), Equation 22. However, a new view factor ($F_{2R}$) to determine the amount of radiation received by the adjoining bulkhead is calculated as perpendicular plates with a common edge [Ref. 4].

$$F_{2R}=\frac{1+\left(\frac{w_2}{w_R}\right)-\left[1+\left(\frac{w_2}{w_R}\right)^2\right]^{\left(\frac{1}{2}\right)}}{2} \tag{29}$$

These equations are solved as previously discussed. A schematic of the surface radiation resistances is given in Figure 7.

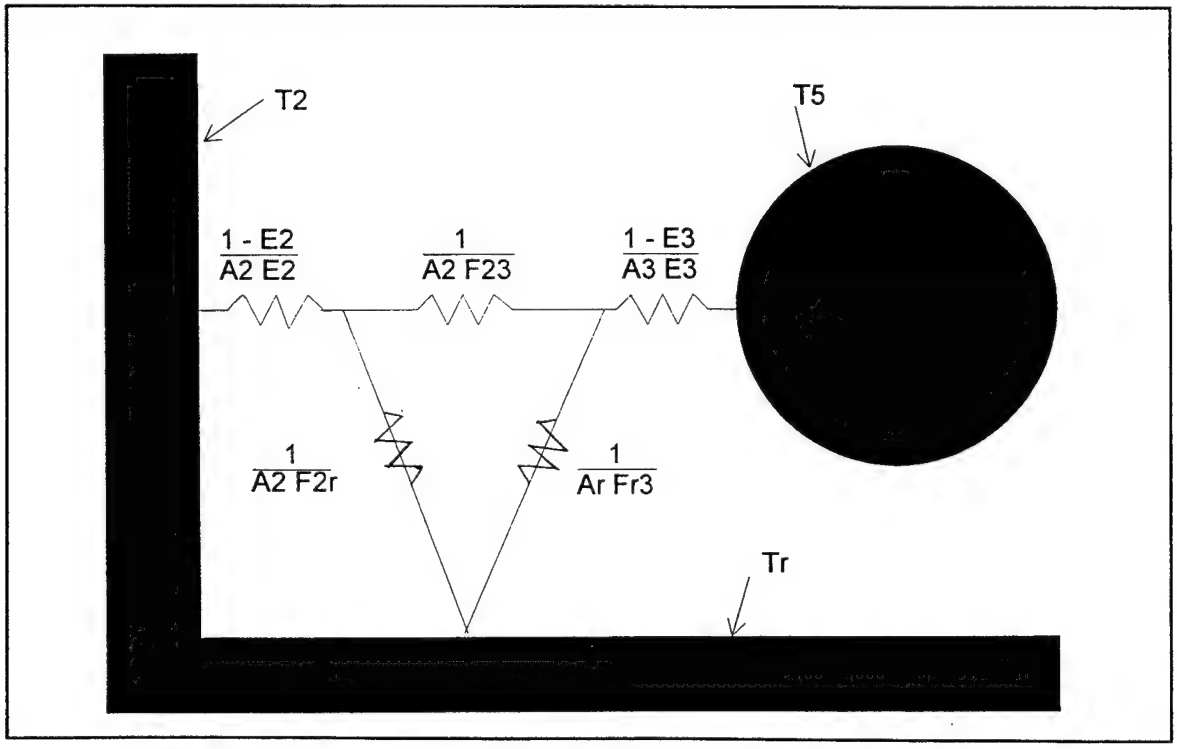


Figure 7. 1st Air Space Resistance Network (Reradiating Surface).

## 4. Finite Difference Equations

The capacitance and transferred thermal energy from conduction and the effects of convection and radiation are combined to form a set of explicit finite difference equations to solve for the temperature at each node in the thermal resistance network. Each is solved simultaneously at each instant in time, which is defined by the time step specified in the algorithm. These finite difference equations were derived by conducting an energy balance about each temperature node. Because this is a time dependent model due to the capacitance in the solid material of the bulkhead, canister walls and missile, the thermal energy stored in the solid material is taken into account in the energy balance.

$$\dot{E}_{in}=\dot{E}_{stored} \tag{30}$$

All heat flow is assumed to flow into the node, and that each node in the resistance network is initially at ambient conditions (300 K). The result of the energy balance yields equations for the nodal temperature at a time increment.

$$T_2(p+1)=2\left[\frac{\Delta t}{\rho c A\Delta x}\left(\frac{T_1(p)-T_2(p)}{R1_{cond}}\right)+\frac{\Delta t}{\rho c A\Delta x}\left(\frac{T_3(p)-T_2(p)}{R_t}\right)+\left(\frac{T_1(p)+T_2(p)}{2}\right)\right]-T_1(p+1) \tag{31}$$

$$T_3(p+1)=2\left[\frac{\Delta t}{\rho c A\Delta x}\left(\frac{T_2(p)-T_3(p)}{R_t}\right)+\frac{\Delta t}{\rho c A\Delta x}\left(\frac{T_4(p)-T_3(p)}{R2_{cond}}\right)+\left(\frac{T_3(p)+T_4(p)}{2}\right)\right]-T_4(p+1) \tag{32}$$

$$T_4(p+1)=2\left[\frac{\Delta t}{\rho cA\Delta x}\left(\frac{T_3(p)-T_4(p)}{R2_{cond}}\right)+\frac{\Delta t}{\rho cA\Delta x}\left(\frac{T_5(p)-T_4(p)}{R2_t}\right)+\left(\frac{T_3(p)+T_4(p)}{2}\right)\right]-T_3(p+1) \quad \textbf{(33)}$$

$$T_5(p+1)=2\left[\frac{\Delta t}{\rho cA\Delta x}\left(\frac{T_4(p)-T_5(p)}{R2_t}\right)+\frac{\Delta t}{\rho cA\Delta x}\left(\frac{T_6(p)-T_5(p)}{R3_{cond}}\right)+\left(\frac{T_5(p)+T_6(p)}{2}\right)\right]-T_6(p+1) \quad \textbf{(34)}$$

$$T_6(p+1)=2\left[\frac{\Delta t}{\rho cA\Delta x}\left(\frac{T_5(p)-T_6(p)}{R3_{cond}}\right)+\frac{\Delta t}{\rho cA\Delta x}\left(\frac{T_7(p)-T_6(p)}{R3_t}\right)+\left(\frac{T_5(p)+T_6(p)}{2}\right)\right]-T_5(p+1) \quad \textbf{(35)}$$

$$T_7(p+1)=2\left[\frac{\Delta t}{\rho cA\Delta x}\left(\frac{T_6(p)-T_7(p)}{R3_t}\right)+\frac{\Delta t}{\rho cA\Delta x}\left(\frac{T_8(p)-T_7(p)}{R4_{cond}}\right)+\left(\frac{T_7(p)+T_8(p)}{2}\right)\right]-T_8(p+1) \quad \textbf{(36)}$$

$$T_8(p+1)=2\left[\frac{\Delta t}{\rho cA\Delta x}\left(\frac{T_7(p)-T_8(p)}{R4_{cond}}\right)+\left(\frac{T_7(p)+T_8(p)}{2}\right)\right]-T_7(p+1) \quad \textbf{(37)}$$

## B. LIMITATIONS

In the construction of this model, a high level of accuracy was not anticipated due to its one dimensionality. However, the goal is to develop a model that achieves moderately accurate solutions to provide baseline data on the cook-off of Tomahawk missiles contained in a CCL magazine. The primary limitations and associated errors with

this model are in the finite-differencing method, thermophysical property data, geometric assumptions, and simplification of the heat transfer process.

## 1. Finite Difference Method

The finite difference solution used is the explicit method. In this solution method, the unknown nodal temperatures for the new (p+1) time are determined from known nodal temperatures at the previous (p) time. The accuracy of this method depends on the distance between nodes ($\Delta x$) and the time step ($\Delta t$), as these values decrease the accuracy of the solution increases. The distance between nodes is chosen based on the geometry of the model, and the time step is chosen based on the stability requirements. The difficulty with the explicit method is that it is not unconditionally stable. This condition is characterized by oscillations which diverge from a steady value instead of converging as anticipated in transient conduction problems. To determine the time step at which the algorithm used in the model is stable, the following criterion for a one dimensional node is solved for $\Delta t$.

$$Fo = \frac{\alpha \Delta t}{(\Delta x)^2} = \frac{1}{2} \tag{38}$$

The limiting time step in this model is governed by the inner cylinder wall based on its values of wall thickness ($\Delta x$) and thermal diffusivity ($\alpha$). Therefore, maximum allowable time step is 0.37 seconds. The more the time step is reduced below 0.37 seconds, the more accurate the solution. However, the number of iterations to achieve the desired time

span increases rapidly and makes it computationally intensive. Therefore, 0.37 seconds is used in all calculations to optimize the computing time.

## 2. Property Data

The thermophysical properties obtained from Touloukian [Ref. 6], which are entering arguments throughout the algorithm, are a large source of error. Not only is there a error associated with curve fitting of the data, but also in the experimental procedure in obtaining the properties. The error reported by Touloukian [Ref. 6] in the experimental procedures used to obtain the thermophysical property data of the substances used in the CCL are listed in Table 1.

| EXPERIMENTAL ERROR | | | |
|---|---|---|---|
| | STEEL | TITANIUM | AIR |
| Specific Heat (cp) | 4% | 0.2% | n/a |
| Thermal Conductivity (k) | 1% | 5-15% | 1-5% |
| Emissivity ($\varepsilon$) | 2% | 8% | n/a |
| Thermal Diffusivity ($\alpha$) | 5-10% | 10% | n/a |
| Kinematic Viscosity ($\nu$) | n/a | n/a | 2% |

Table 1. Experimental Error in the Measurement of Thermophysical Properties.

In order for the algorithm to evaluate the properties of the metals and air, a curve fit or regression was conducted on the data. In this procedure, a curve was developed that 'best fits" the data but does not necessarily pass through the data points. The "best fit" or least squares curve fitting seeks to minimize the sum of the squared error. The error is the distance between the polynomial curve and the actual data point. Squaring this distance at

each data point and adding the squared distances together is the sum of the squared error. Therefore, the curve generated by the polynomial is the curve that makes the sum of the errors as small as it can be, "best fit" [Ref. 8]. The error in relation to the data and the polynomial generated by the curve fit was less than ten percent in all cases, which is within the range of the experimental data error.

## 3. Geometry

In the modeling of the CCL each geometric shape is considered to be solid polished material with no attachments. Obvious architecture with respect to a functioning weapon system have been neglected such as wire ways, electronic packaging, supporting frame work, etc.

Several assumptions have been made with respect to radiation. The metal on all surfaces throughout the model are assumed to be unpainted and polished. Thus, the emissivity is assumed to be much higher than that of a painted surface. Additionally, the model accounts only for the heat emitted from the bulkhead to the modeled CCL and neglects radiation effects from the surrounding canisters. Finally, radiation with respect to the other walls in the room on fire to the CCL bulkhead is neglected, as well as, the convective resistance on the outer surface of the bulkhead.

The final assumption in the model is that the missile has the properties of aluminum and is solid throughout. The missile electronics and cabling are neglected. Aluminum was chosen because it is used consistently throughout the missile. Its property data would provide a good assumption as to how the missile reacts to the heat energy absorbed and provide a temperature profile at the center of the missile.

# III. FIRE SCENARIOS

To develop accurate time-temperature profiles describing the heat-up rate of the CCL, credible fire scenarios are identified based on the type of combustible material fueling the fire and its probable intensity. Four scenarios are analyzed by the CCL heat transfer model to achieve a good understanding of how the CCL's heat-up rate will differ when exposed to different types of fires.

The first scenario analyzed consisted of a compartment fire involving common shipboard fuels (JP-5, JP-4, F-76, etc). The time-temperature profile is characterized by a increase in temperature from ambient conditions to 2000°F (1366 K) over a period of five minutes and is then maintained at the maximum temperature for the duration of the fire [Ref. 1]. This scenario is typically used to evaluate the structural integrity of the effected space both during and after the fire [Ref. 11].

The second fire scenario is typically used in modeling fires fueled by common combustible material, such as a berthing compartment fire. The time-temperature profile is characterized by a increase in temperature from ambient conditions to 1700°F (1200 K) over a period of fifteen minutes, and then maintains a steady temperature rise of 84°F/hour (46 K/hour) [Ref. 11].

A fire fueled by a missile's residual solid propellant, as experienced by the USS STARK (FFG 31), is the most intense and is the next scenario analyzed. Propellant fires are normally short lived but can reach temperatures in excess of 3000°F (1922 K). For the purpose of this scenario, it is assumed that maximum temperature is reached in thirty seconds, and that the temperature is then maintained until the self-ignition temperature of the missile's solid propellant is reached.

The last scenario analyzed was developed by the U. S. Navy's Insensitive Munitions (IM) Program to characterize the thermal response of munitions exposed to slow cook-off conditions. The slow cook-off condition is described by a temperature rise of 6°F/hour (3.33 K/hour) [Ref. 1].

The IM Program also developed a fire scenario to describe fast cook-off, that immerses the missile in a JP-5 pool fire in which the average temperature must be at or above 1600°F [Ref. 1]. This scenario is most likely on ordnance stored on a flight deck rather than a missile contained in a CCL magazine. Therefore, the fast cook-off scenario is not analyzed.

The test data from the Insensitive Munitions program shows that the missile's solid propellant motor (MK 106 Booster) and explosives will self-ignite between 300 and 400°F (422 and 478 K), and the liquid propellant motor, fueled by JP-10 or RJ-4, can self-ignite at temperatures as low as 460°F (511 K). Depending on the rate of temperature increase, self-ignition of the energetic material can range from a slow burn to an immediate deflagration. [Ref. 1]

Table 2 summarizes the aforementioned fire scenarios and assigns a scenario number. This number is used to refer to the various fire scenarios throughout the rest of the text.

| FIRE SCENARIOS | | |
|---|---|---|
| SCENARIO # | MAXIMUM TEMPERATURE (K) | RATE OF TEMP INCREASE |
| 1 | 1366 | 3.55 K/second |
| 2 | n/a | 80 K/min < 1186 K<br>0.77 K/min > 1186 K |
| 3 | 1922 | 54.07 K/second |
| 4 | n/a | 3.33 K/hour |

Table 2. Fire Scenarios.

# IV. RESULTS

As mentioned in the objectives, this study models two CCLs within the ship's weapon module. The first is located in the first row along the centerline of the ship, and the second is the corner CCL in which the adjacent wall is considered a reradiating surface. The four fire scenarios mentioned in the previous chapter are analyzed for each CCL location. Additionally, each scenario is conducted twice. The first solves for surface radiative resistance explicitly and the second with a Taylor series expansion. After the scenario number, the explicit method and Taylor series expansion methods will be denoted by the letter (A) and (B), respectively.

The temperature range in which the missile's components, specifically the warhead and solid propellant motor, will self-ignite is between 422 and 478 K. The liquid propellant will self-ignite as low as 511 K. The times to reach these temperatures for the center and corner CCL are listed in Table 3 and 4, respectively. Time-temperature profiles are plotted in Figures 8 through 15 for the center CCL and Figures 16 through 23 for the corner CCL.

The two methods used to determine the surface radiation, described in Chapter II, are compared because of the large differences experienced in each scenario's time-temperature profiles. The Taylor series expansion produces two types of error, truncation and round-off. The truncation error is due to the approximation formula. In general, increasing the order of the Taylor series reduces the truncation error but increases the round-off error. For this model both types of errors are probably high for two reasons:

the expansion was only carried out to the first derivative to reduce the amount of computations, and the round off error is high due to the curve fitted thermophysical properties used throughout the model. Solving for the surface radiative resistance explicitly eliminates the truncation error, however, it is still affected by the round off error. Solving for the surface radiative resistances with a Taylor series expansion produces a more conservative time-temperature profile, and is the recommended method.

| TIME TO COOK-OFF | | | |
|---|---|---|---|
| SCENARIO # | TIME TO REACH 511 K (min) | TIME TO REACH 422-478 K (min) | ASSOCIATED FIGURE |
| 1A | 204.42 | 141.06-181.02 | 8 |
| 1B | 152.26 | 108.48-136.32 | 9 |
| 2A | 254.40 | 187.52-230.96 | 10 |
| 2B | 198.68 | 147.43-180.73 | 11 |
| 3A | 64.85 | 49.71-59.28 | 12 |
| 3B | 53.25 | 42.23-49.25 | 13 |
| 4A | inf | inf | 14 |
| 4B | inf | inf | 15 |

Table 3. Cook-Off Times for Scenarios (Center CCL).

| TIME TO COOK-OFF | | | |
|---|---|---|---|
| SCENARIO # | TIME TO REACH 511 K (min) | TIME TO REACH 422-478 K (min) | ASSOCIATED FIGURE |
| 1A | 199.88 | 137.76-176.95 | 16 |
| 1B | 149.59 | 106.43-133.88 | 17 |
| 2A | 250.04 | 183.92-226.88 | 18 |
| 2B | 195.83 | 145.02-178.03 | 19 |
| 3A | 63.50 | 48.67-58.06 | 20 |
| 3B | 52.42 | 41.56-48.48 | 21 |
| 4A | inf | inf | 22 |
| 4B | inf | inf | 23 |

Table 4. Cook-Off Times for Scenarios (Corner CCL).

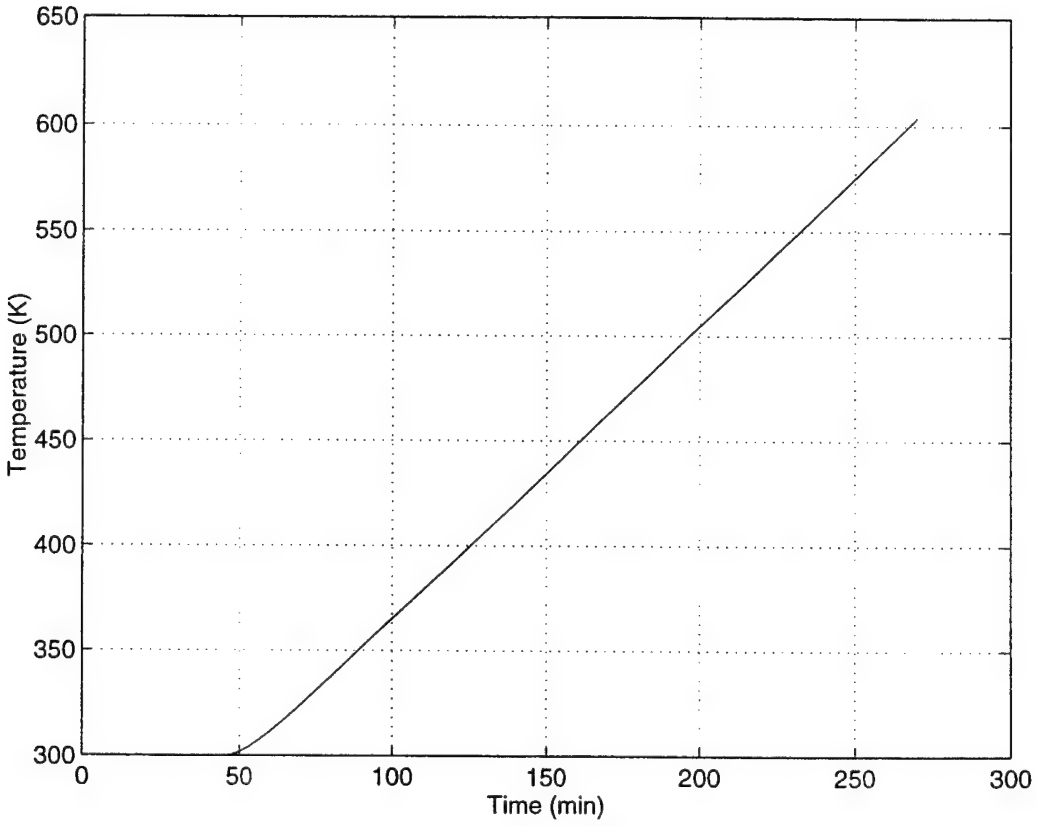


Figure 8. Scenario 1A-Missile Heat-Up Rate.

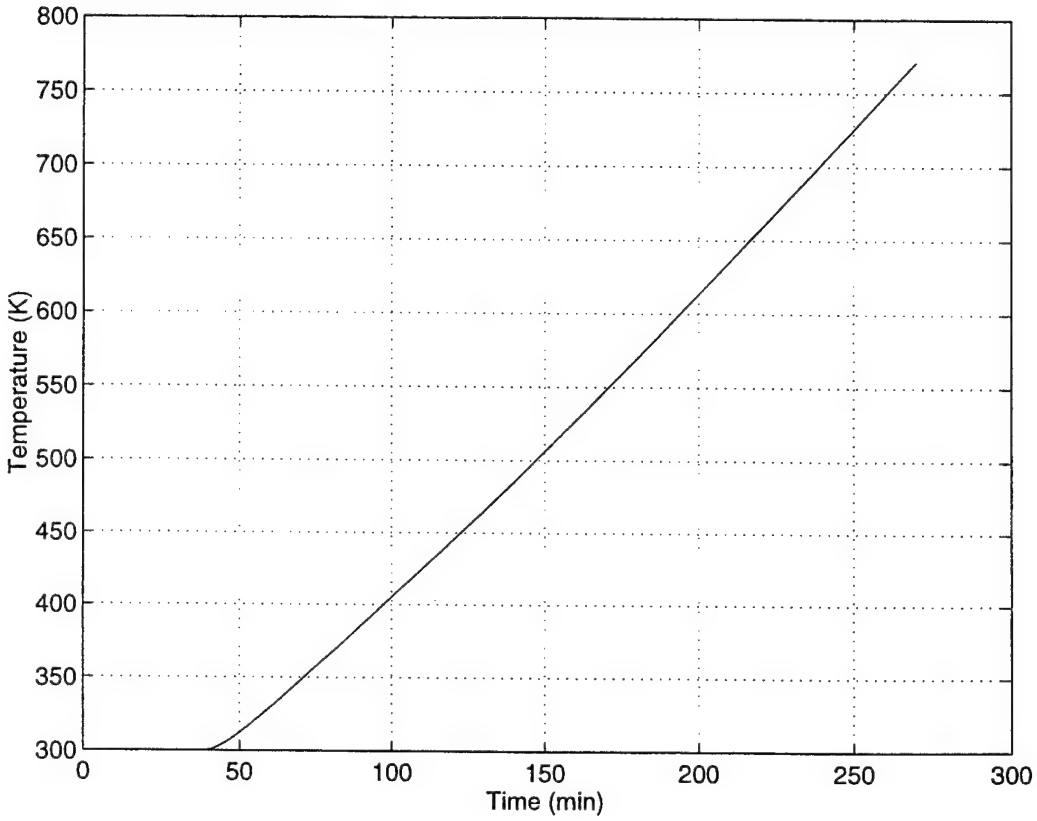


Figure 9. Scenario 1B-Missile Heat-Up Rate.

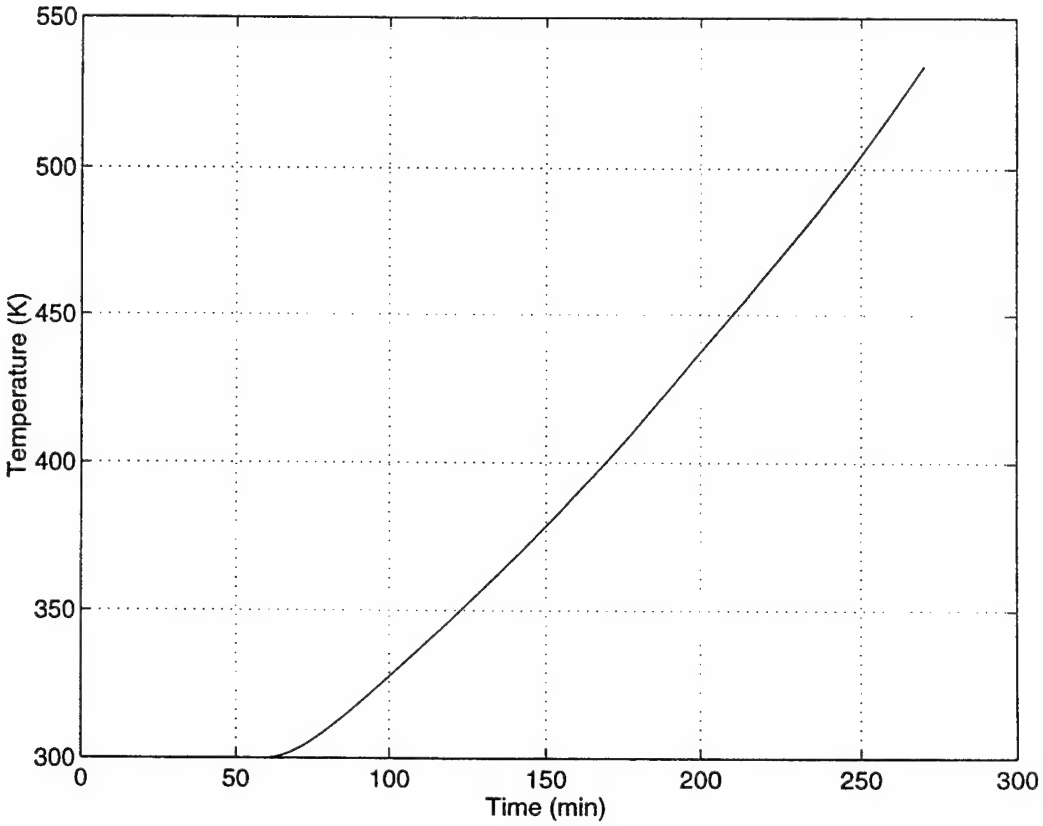


Figure 10. Scenario 2A-Missile Heat-Up Rate.

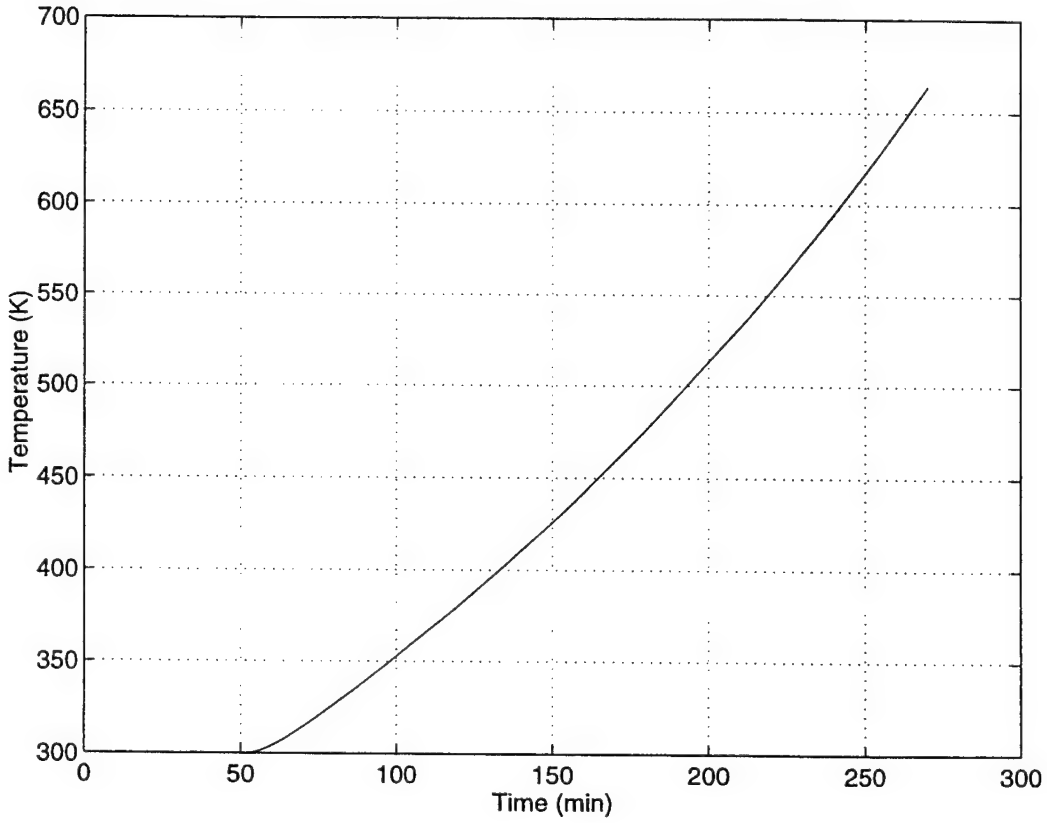


Figure 11. Scenario 2B-Missile Heat-Up Rate.

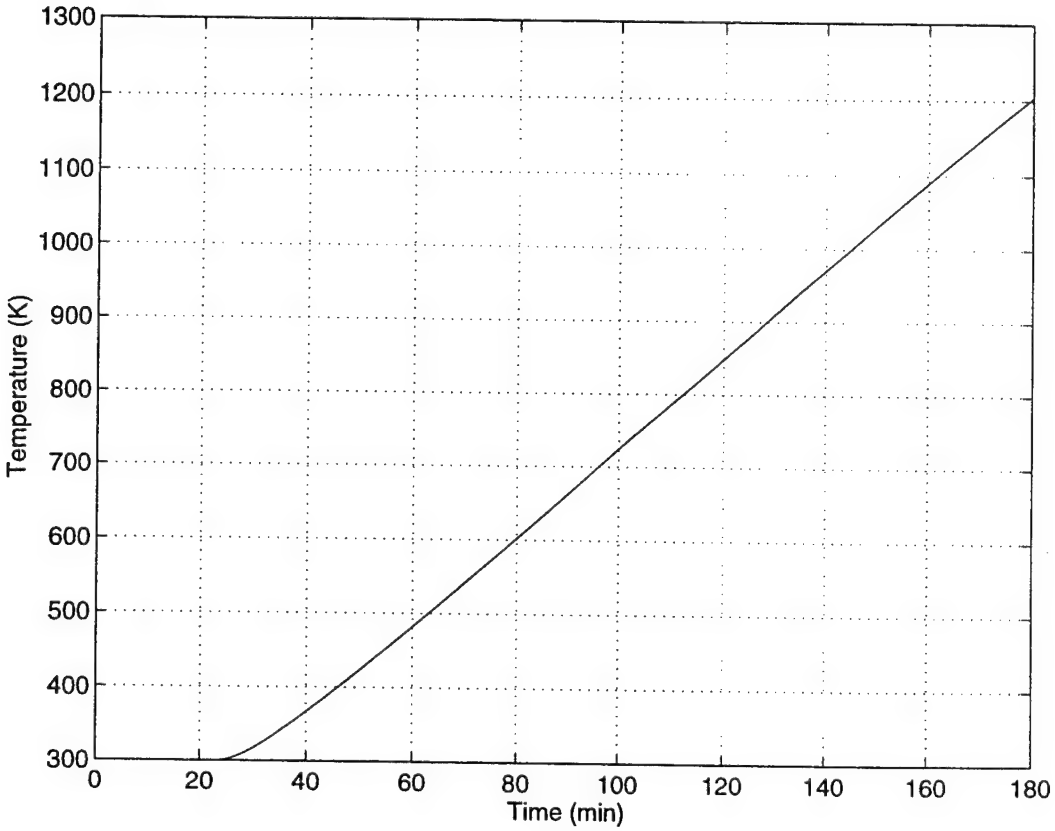


Figure 12. Scenario 3A-Missile Heat-Up Rate.

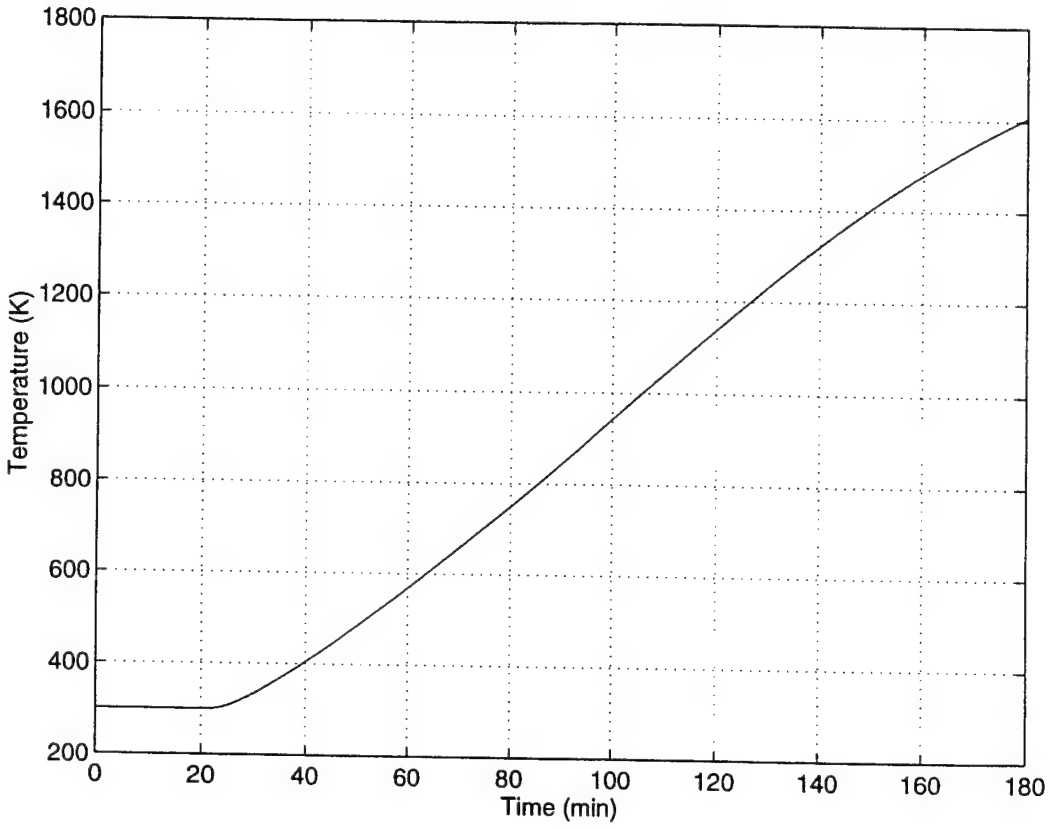


Figure 13. Scenario 3B-Missile Heat-Up Rate.

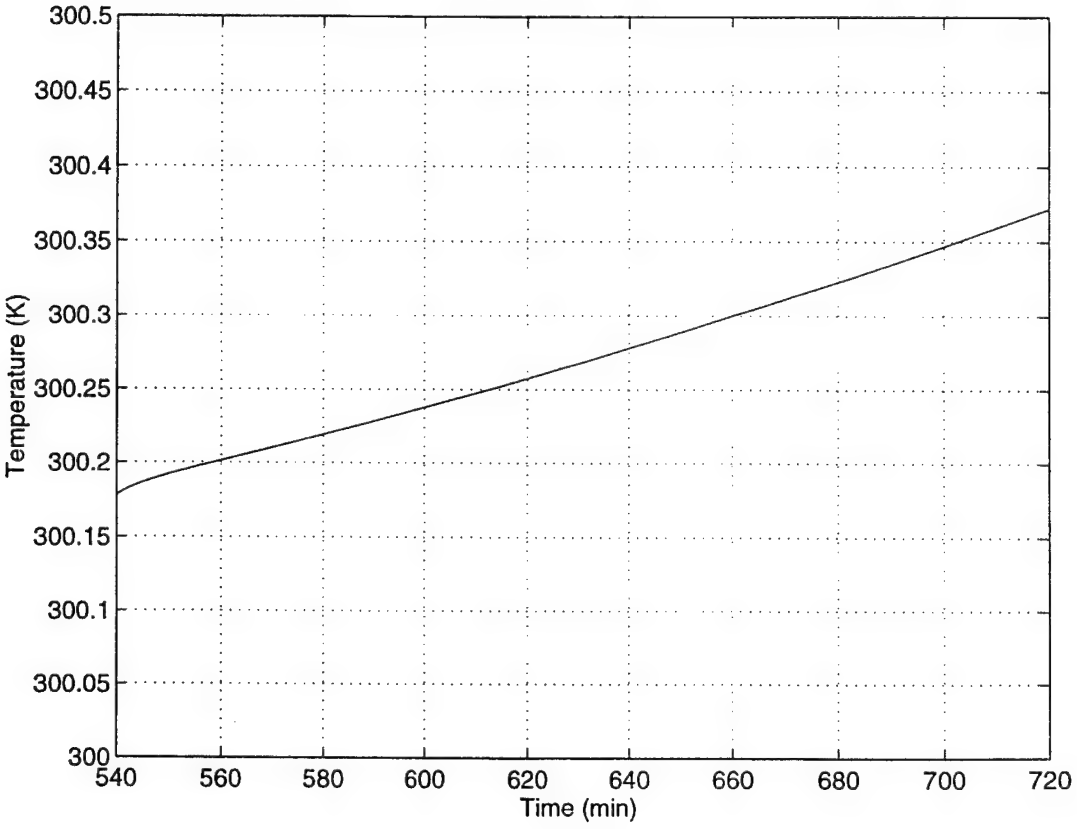


Figure 14. Scenario 4A-Missile Heat-Up Rate.

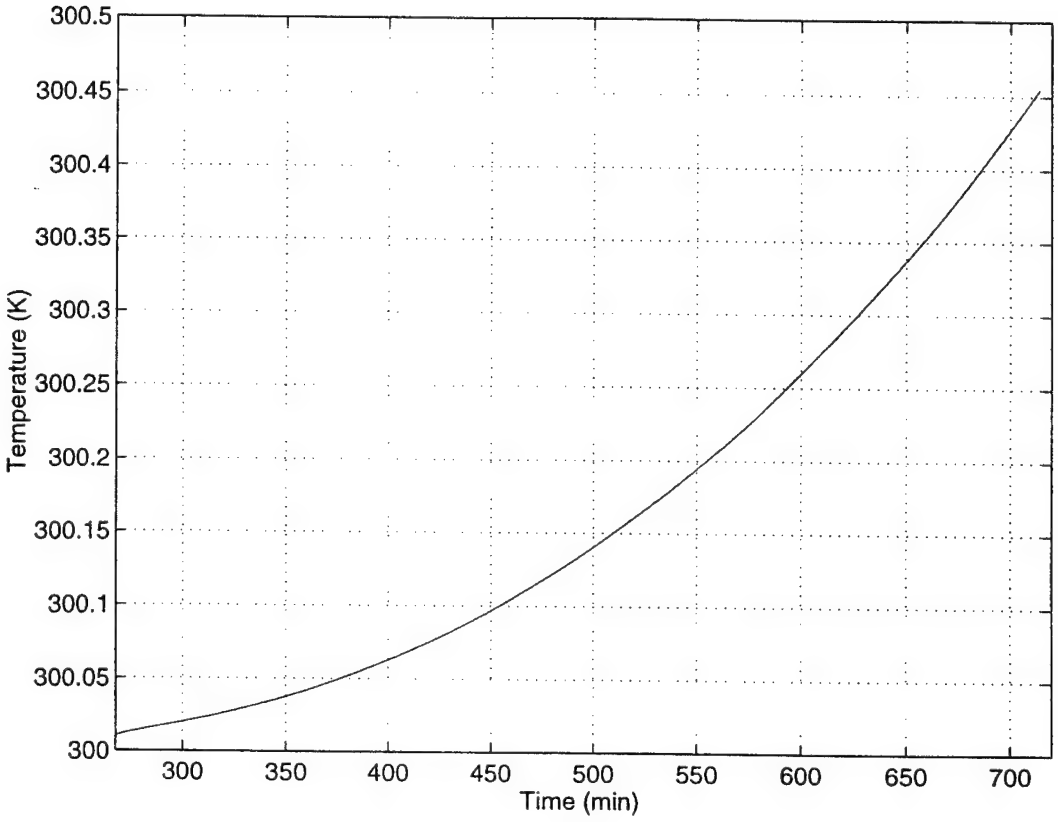


Figure 15. Scenario 4B-Missile Heat-Up Rate.

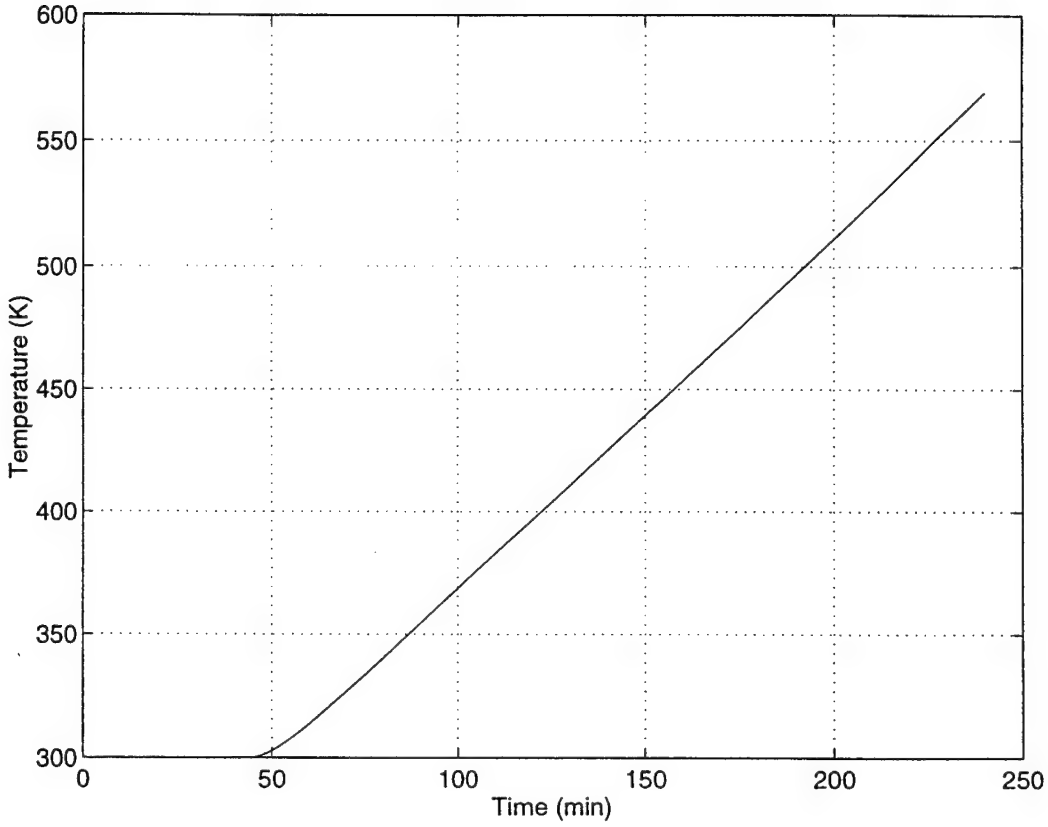


Figure 16. Scenario 1A-Missile Heat-Up Rate w/ Reradiating Surface.

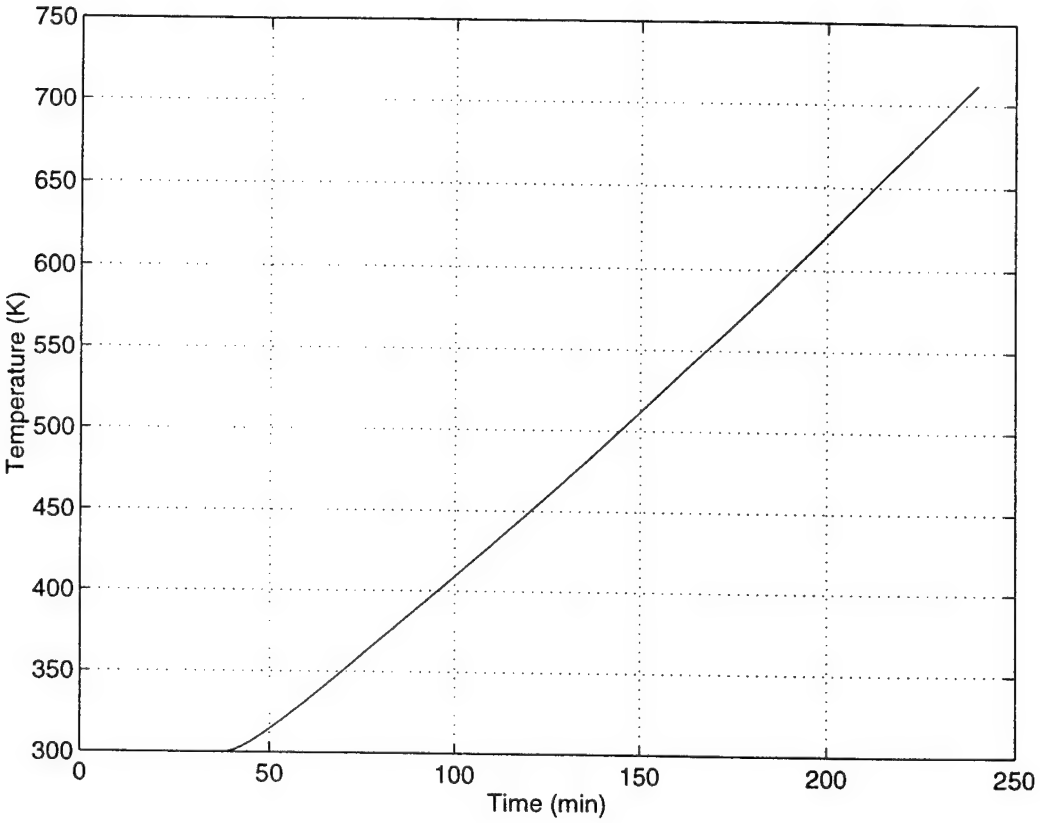


Figure 17. Scenario 1B-Missile Heat-Up Rate w/ Reradiating Surface.

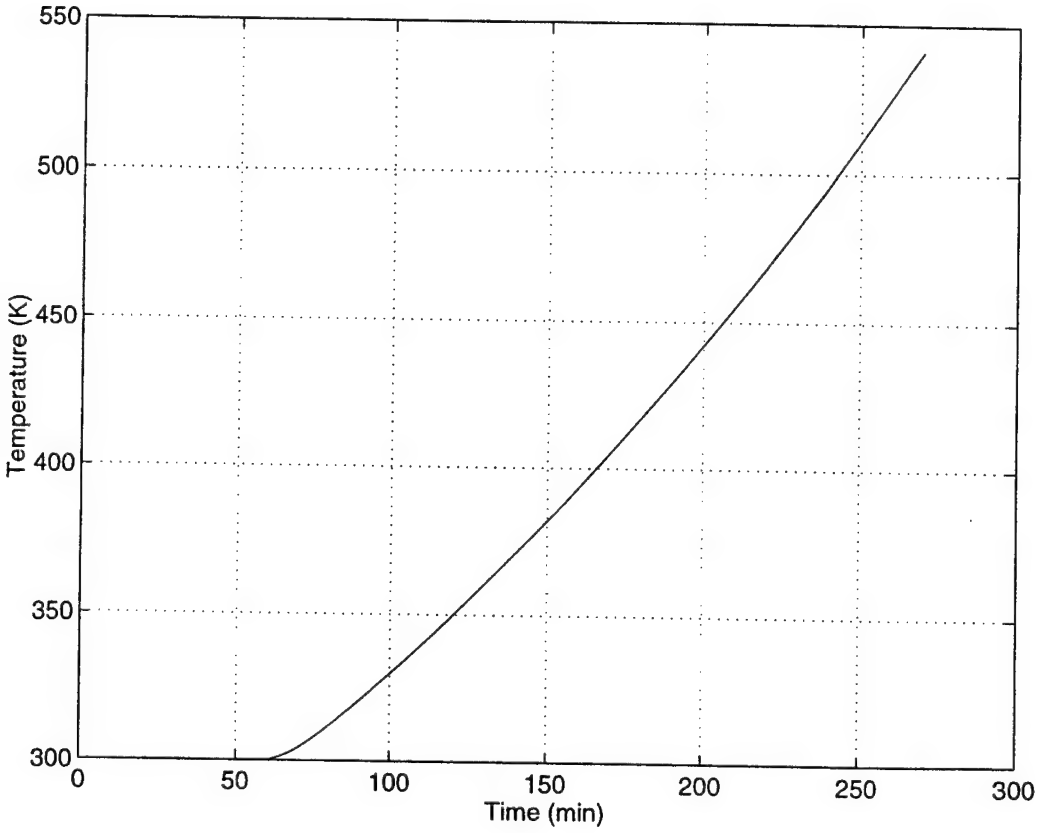


Figure 18. Scenario 2A-Missile Heat-Up Rate w/ Reradiating Surface.

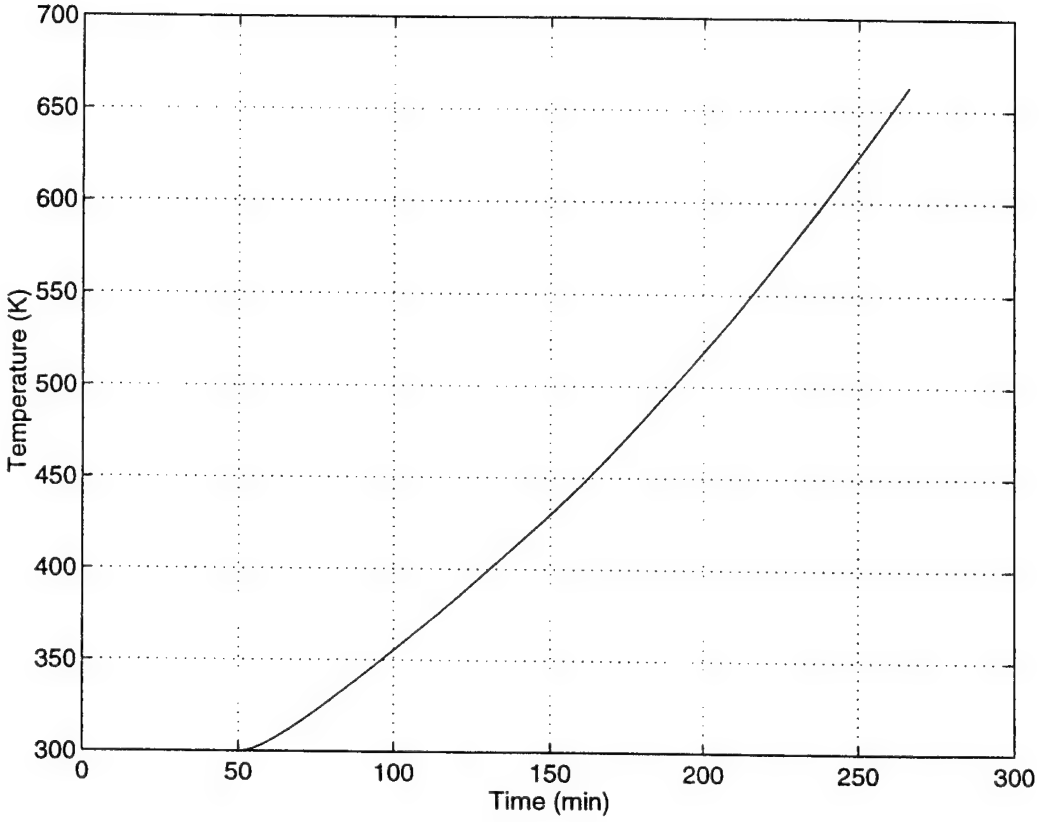


Figure 19. Scenario 2B-Missile Heat-Up Rate w/ Reradiating Surface.

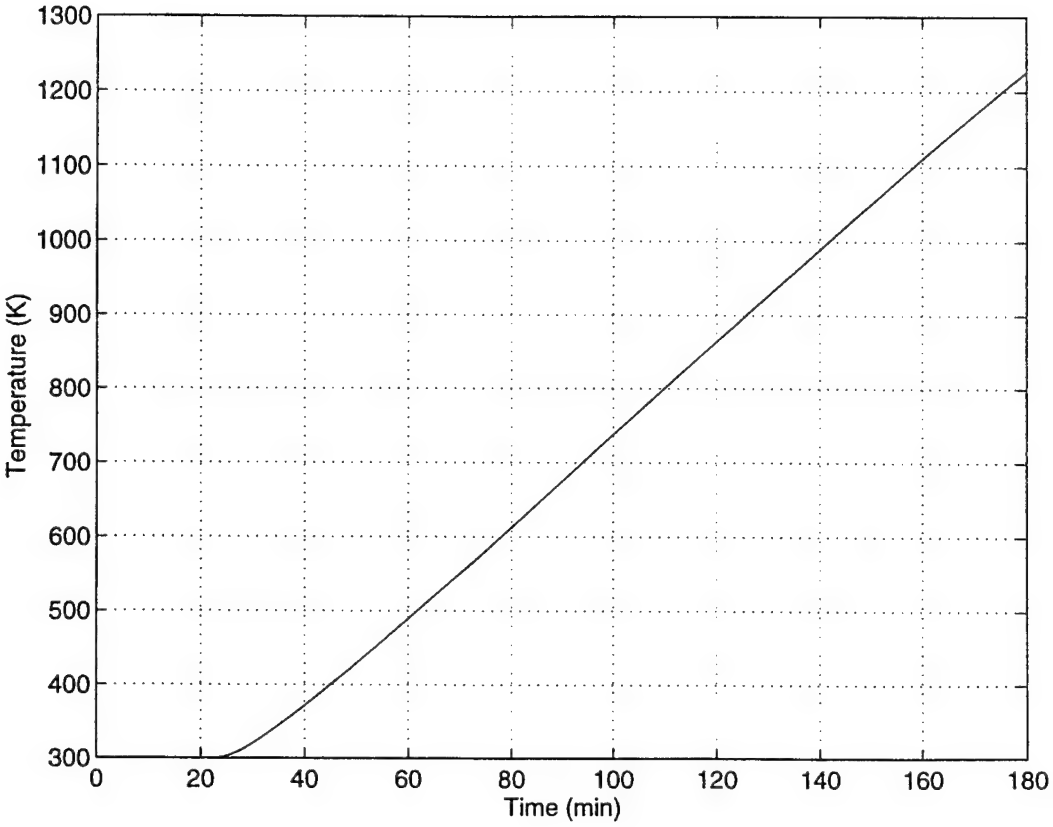


Figure 20. Scenario 3A-Missile Heat-Up Rate w/ Reradiating Surface.

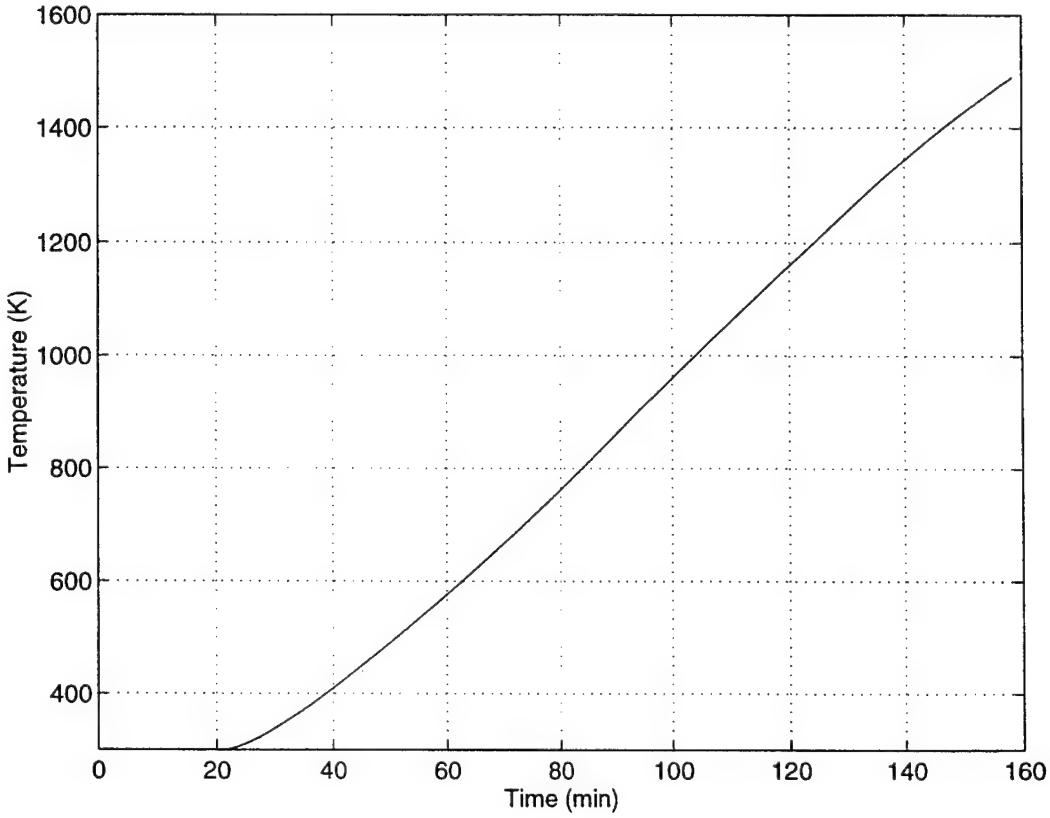


Figure 21. Scenario 3B-Missile Heat-Up Rate w/ Reradiating Surface.

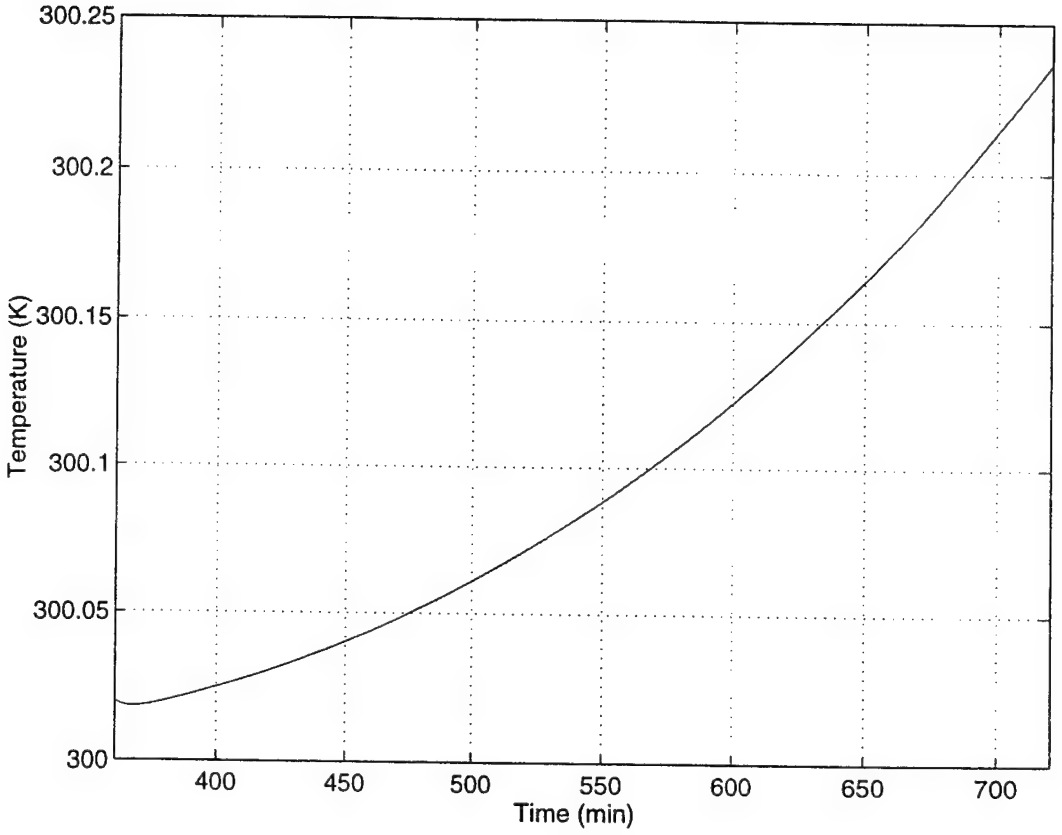


Figure 22. Scenario 4A-Missile Heat-Up Rate w/ Reradiating Surface.

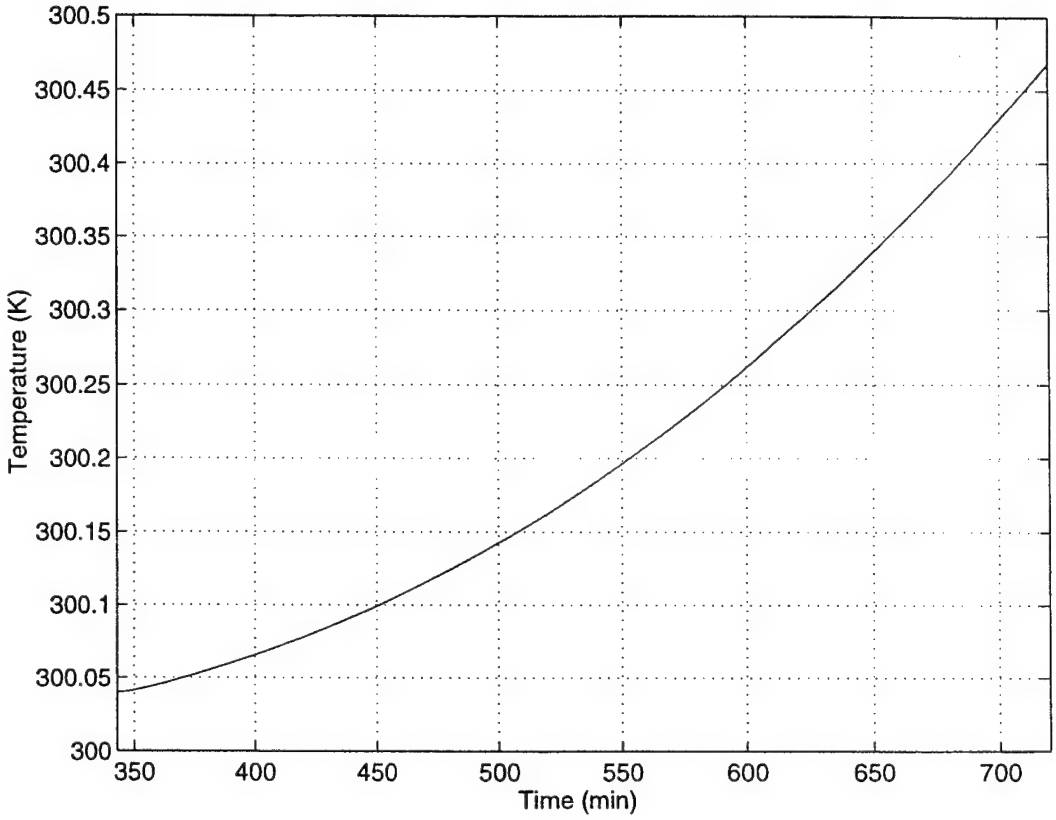


Figure 23. Scenario 4B-Missile Heat-Up Rate w/ Reradiating Surface.

# V. CONCLUSIONS

The fire scenarios analyzed by the CCL heat transfer model in this study showed that the CCL can withstand an intense conflagration if the bulkheads surrounding the magazine remain intact. In the most intense fire situation, Scenario 3, ship's personnel have approximately forty-five minutes to gain control of the fire or cool the weapons in the magazine prior to cook-off. Conceivably, automated fire protection equipment could increase the amount of time firefighters have to control the fire without the immediate hazard of cook-off.

In its current stage of development, the CCL's installed fire protection features have not been designed. However, the uniqueness of the CCL module will require some changes, as compared to the fire protection equipment currently installed in the MK 41 VLS. The MK 41 VLS fire protection system consist of a deluge system installed in the canister designed to cool the missile in the event of an inadvertent motor ignition or extreme over temperature situation, and a sprinkling system designed to provide cooling external to its canisters should it sense a rapid temperature rise [Ref. 1]. Because the CCL acts both as a launcher and transport device, introducing a fire protection system into the CCL will hamper its primary advantage of being a totally integrated package.

A possible alternative to the current deluge system would be a similar system of two or more mounted spray nozzles directed to impinge the canister at the top outer surface of the CCL providing a cooling film around the entire canister but not wetting the missile. In addition to the outer deluge system, a magazine sprinkler should also be installed to cool the entire magazine should temperatures increase too rapidly. The advantages of keeping the fire protection system outside of the CCL are two fold;

- If there is an inadvertent sprinkling of the magazine or activation of the deluge system, the missile is not effected by the water and the costly process of sending the weapon to a rework facility for repairs and recertification or decertification and dismantling is avoided. It is possible that after a incident of this type onboard data transmission, continuity and accuracy checks can be conducted to verify the missile is fully functional after the module and electrical connections are cleaned.

- The second advantage, and most important, is to maintain the ease of the installation and removal process from the ship's weapon module. Installing piping connections for a deluge system, which of course will have to meet high shock criteria, will make a relatively easy installation/removal operation much more cumbersome.

The disadvantage of water systems is the generation of steam in intense fires resulting in a steam explosion. There are other types of systems, such as inert gas fire protection systems, which may be worthy of investigation. But when dealing with intense fires with long durations, as in the USS STARK, the availability and cooling effects of seawater proved to be effective. Investigating the installation of a relief system should steam accumulate in the module during a fire is recommended.

Another characteristic of missile solid propellent, brought to our attention by NAVAIR, China Lake, which warrants mentioning, is that prior to reaching self-ignition temperature, the propellant begins to off-gas some of its volatile materials [Ref. 11]. The temperature at which this occurs is yet to be identified. From the standpoint of any exposure to an over-temperature situation, a missile may be damaged even if cook-off did not occur. However, an interesting side effect was noticed that if the solid propellant was remixed after the off gassing, it burned longer and with less thermal energy. Follow on research is recommended to determine at what temperature the solid propellent begins to off-gas.

In general, this study will provide CCL project managers and designers with baseline time-temperature profiles to make decisions concerning the construction and survivability of the CCL launching system, especially with respect to installed fire protection systems. Additionally, it will provide ship's personnel with a conservative missile cook-off time based on the type of fire, so that the damage control situation can be assessed and priorities set.

# VI. RECOMMENDATIONS

In any continuation of this study the following are recommended:

- The CCLs modeled are sized for Tomahawk missiles and are the same throughout the ship's weapon module. Future studies should model the ship's weapon module for an actual deployment weapon configuration in which different types of CCLs carry a variety of weapons in support of all the ship's mission areas.

- Build a user interface at the MATLAB command window to easily vary the fire scenario. Currently, to vary the fire scenarios the computer code must be modified.

- Account for surface radiation from other CCLs in the magazine.

- Utilize temperature data from fire scenarios currently being conducted in the ex-USS SHADWELL. This should provide more accurate data and a larger variety of fire curves to be evaluated by the CCL Fire Model.

# APPENDIX A. CCL-FIRE PROGRAM CODE (2A-CENTER)

This MATLAB code solves for radiation explicitly as described in the radiation section of Chapter II. This code is set up for the center CCL and scenario 2.

```
format bank
clear

% DIMENSIONS FOR CANISTERS & SURROUNDING VLS WALL.

w=1;              % [m] Width of for and aft bulkhead.
Lw=1;             % [m] Height of wall surrounding CCL module.
Lc=1;             % [m] Height of inner/outer canister wall.
Lm=1;             % [m] Length of missile.
delx=0.0048;      % [m] Thickness of wall surrounding CCL module.
r=0.00159;        % [m] Near center of missile (1/16 in).
ro=0.2586;        % [m] Radius of missile.
r1=0.2635;        % [m] Inside radius of inner cylinder wall.
r2=0.2667;        % [m] Outside radius of inner cylinder wall.
r3=0.3492;        % [m] Inside radius of outer cylinder wall.
r4=0.3571;        % [m] Outside radius of outer cylinder wall.
s=0.8382;         % [m] Distance between cylinder CL.
g=9.81;           % [m/s^2] Gravitational constant.
sig=5.67e-008;    % [W/m^2*K^4] Stefan-Boltzmann constant.
A1=w*Lw;          % [m^2]Area of VLS wall perp to dir of heat flux.
A2=A1;
A3=2*pi*r4*Lc;    % [m^2] Outer surface area of 1st cylinder.
A4=2*pi*r3*Lc;    % [m^2] Inner surface area of 1st cylinder.
A5=2*pi*r2*Lc;    % [m^2] Outer surface area of 2nd cylinder.
A6=2*pi*r1*Lc;    % [m^2] Inner surface area of 2nd cylinder.
A7=2*pi*ro*Lc;    % [m^2] Surface area of missile.
V1=delx*w*Lw;
V2=pi*Lc*(r4^2-r3^2);
V3=pi*Lc*(r2^2-r1^2);
V4=pi*ro^2*Lm;


% [K]  INITIAL AMBIENT CONDITIONS TO START ITERATION.

T2(1)=300;
T3(1)=300;
```

```
T4(1)=300;
T5(1)=300;
T6(1)=300;
T7(1)=300;
T8(1)=300;


% DEFINES TIME STEP AND NUMBER OF ITERATIONS

S=50000;      %      Number of iterations.
delt=0.36;    %  [s] Time step.


% BEGINS LOOP TO SOLVE FOR ALL TEMPS IN RESISTANCE NETWORK.

for p=1:S
p1=p

% [s] Time.
t(p)=(delt*(p-1));

dT(p)=t(p)*1.3333;
dTA(p)=t(p)*0.0128;
T1(p)=300+dT(p);
T1A(p)=1200+dTA(p);

if T1(p)<=1200
T1(p)=T1(p);
else
T1(p)=T1A(p);
end

t(p+1)=(delt*(p));
dT(p+1)=t(p+1)*1.3333;
dTA(p+1)=t(p+1)*0.0128;
T1(p+1)=300+dT(p+1);
T1A(p+1)=1200+dTA(p+1);

if T1(p+1)<=1200
T1(p+1)=T1(p+1);
else
T1(p+1)=T1A(p+1);
end
```

```
%%%  SOLVES SECTION 1 [T2] %%%

% [K] Film temperature to evaluate properties of mild steel
Tf1(p)=(T1(p)+T2(p))/2;

% [W/m*K] Thermal conductivity of bulkhead.
kw1(p)=abs((1.8869e-005*Tf1(p)^2)-(6.9896e-002*Tf1(p))+83.438);

% [J/kg*K] Specific Heat of bulkhead.
cp1(p)=abs(((-2.2828e-006)*Tf1(p)^3)+((4.6812e-003)*Tf1(p)^2)-(2.3469*Tf1(p))+800.
99);

% [m^2/s] Thermal diffusivity of bulkhead.
alf1(p)=abs(((4.0118e-014)*Tf1(p)^3)-((7.9337e-011)*Tf1(p)^2)+(3.3733e-008*Tf1(p))
+1.0388e-005);

% [kg/m^3] Density of bulkhead.
rho1(p)=kw1(p)/(cp1(p)*alf1(p));

% Solves for the conductive resistance in bulkhead.
Rc1(p)=delx/(kw1(p)*A2);

% [K] Film temperature to evaluate properties in 1st air space.
Tf2(p)=(T2(p)+T3(p))/2;

% [W/m*K] Thermal conductivity of air.
ka2(p)=abs((4.9198e-011*Tf2(p)^3)-(1.608e-007*Tf2(p)^2)+(2.014e-004*Tf2(p))-0.020
796);

% [m^2/s] Kinematic viscosity of air.
nu2(p)=abs(((7.786e-005*Tf2(p)^2)+(4.4053e-002*Tf2(p))-2.4972)*1.0e-006);

% Prandtl #.
Pr2(p)=abs((-2.5065e-011*Tf2(p)^3)+(8.4944e-008*Tf2(p)^2)-(1.0417e-004*Tf2(p))+0.
74553);


% [K^-1] Exp. Coefficient of air .
B2(p)=1/Tf2(p);

% Emissivity of mild steel.
E2(p)=abs((-9.8416e-008*T2(p)^2)+(2.6912e-004*T2(p))+0.73699);
```

```
% Emissivity of titanium.
E3(p)=abs((-5.0412e-008*T3(p)^2)+(2.4949e-004*T3(p))+0.051504);

% Solves for Rayleigh and Grashof #'s WRT bulkhead inner surface.
Gr2(p)=((g*B2(p)*(T2(p)-Tf2(p))*(Lw^3))/(nu2(p)^2));
Ra2(p)=Gr2(p)*Pr2(p);

% Correlation to solve for the average Nusselt # over a
% vertical flat plat.  Recommended by Churchill and Chu, it is
% good over entire range of Rayleigh #'s.
Nu2(p)=(0.825+((0.387*(Ra2(p)^(1/6)))/((1+((0.492/Pr2(p))^(9/16)))^(8/27))))^2;

% Solves for convective resistance using the average convection
% heat transfer coefficient over the bulkhead inner surface.
h2(p)=Nu2(p)*ka2(p)/Lw;
Rco1a(p)=1/(h2(p)*A2);

% Solves for Rayleigh and Grashof #'s WRT cylinder outer surface.
Gr3(p)=(g*B2(p)*(Tf2(p)-T3(p))*(Lc^3))/(nu2(p)^2);
Ra3(p)=Gr3(p)*Pr2(p);

% IF-THEN LOOP TO DETERMINE IF THE OUTER WALL OF THE CYLINDER
% CAN BE APPROXIMATED AS A PLANE WALL. IF A PLANE WALL
% CHURCHILL
% AND CHU'S CORRELATION FOR A VERTICAL SURFACE IS USED.  IF
% THERE ARE APPRECIABLE CURVATURE EFFECTS A CORRELATION
% DEVELOPED
% BY LE FEVRE AND EDE BASED ON CYLINDER HEIGHT.

if Gr3(p)==0
Nu3(p)=((4/3)*((7*Gr3(p)*Pr2(p)^2)/(5*(20+21*Pr2(p))))^0.25)+((4*Lc*(272+315*Pr2
(p)))/(35*2*r4*(64+63*Pr2(p))));
else
if ((2*r4)/Lc)>=35/(Gr3(p)^1/4)
Nu3(p)=(0.825+((0.387*(Ra3(p)^(1/6)))/((1+((0.492/Pr2(p))^(9/16)))^(8/27))))^2;
else

Nu3(p)=((4/3)*((7*Gr3(p)*Pr2(p)^2)/(5*(20+21*Pr2(p))))^0.25)+((4*Lc*(272+315*Pr2
(p)))/(35*2*r4*(64+63*Pr2(p))));
end
end
```

```
% Solves for convective resistance using the average convection
% heat transfer coefficient over outer surface of the cylinder.
h3(p)=(Nu3(p)*ka2(p))/Lc;
Rco1b(p)=1/(h3(p)*A3);

% Adds convective resistances in series.
Rco1(p)=Rco1a(p)+Rco1b(p);

% Calculates view factor.  Equation from the catalog of radiation
% configuration factors, infinite plane to a row of pipes [C-6].
D=(2*r4)/s;
F23=1-((1-D^2)^0.5)+(D*atan(((1-D^2)/D^2)^0.5));

% Solves the radiative resistance network for two surf enclosure,
% and linearizes the resistance to be used ICW the convective
% resistance.
Rr1(p)=((1-E2(p))/(E2(p)*A2))+(1/(A2*F23))+((1-E3(p))/(E3(p)*A3));
Rrad1(p)= 1/((sig/Rr1(p))*((T2(p)+T3(p))*(T2(p)^2+T3(p)^2)));

% Solves for total resistance, [T3], and begins next iteration.
Rt(p)=(Rco1(p)*Rrad1(p))/(Rrad1(p)+Rco1(p));

% Finite difference equation--explicit method.
H1(p)=delt/(rho1(p)*cp1(p)*V1);
T2(p+1)=2*(((H1(p)/Rc1(p))*(T1(p)-T2(p)))+((H1(p)/Rt(p))*(T3(p)-T2(p)))+((T2(p)+T
1(p))/2))-T1(p+1);

if T2(p+1)<300
T2(p+1)=300;
else
T2(p+1)=T2(p+1);
end


%%% SOLVES SECTION 2 [T3] %%%

% [K] Film temperature to evaluate properties of titanium.
Tf3(p)=(T3(p)+T4(p))/2;

% [W/m*K] Thermal conductivity of canister wall.
kc3(p)=abs((1.7011e-008*Tf3(p)^3)-(4.3316e-005*Tf3(p)^2)+(2.7279e-002*Tf3(p))+20.
358);
```

```
% [J/kg*K] Specific Heat of canister wall.
cp3(p)=abs(((4.6480e-007)*Tf3(p)^3)-((1.4813e-003)*Tf3(p)^2)+(1.5387*Tf3(p))+139.9
3);

% [m^2/s]  Thermal diffusivity of canister wall.
alf3(p)=abs(((-4.532e-015)*Tf3(p)^3)+((1.7281e-011)*Tf3(p)^2)-(1.929e-008*Tf3(p))+1
.3594e-005);

% [kg/m^3] Density of canister wall.
rho3(p)=kc3(p)/(alf3(p)*cp3(p));

% Solves for the conductive resistance through the cylinder wall.
Rc2(p)=log(r4/r3)/(2*pi*kc3(p)*Lc);

% Finite difference equation--explicit method.
H2(p)=delt/(rho3(p)*cp3(p)*V2);
T3(p+1)=2*(((H2(p)/Rt(p))*(T2(p)-T3(p)))+((H2(p)/Rc2(p))*(T4(p)-T3(p)))+((T3(p)+T
4(p))/2))-T4(p);


%%% SOLVES SECTION 3 [T4] %%%

% [K] Film temperature to evaluate air properties in 1st annulus.
Tf4(p)=(T4(p)+T5(p))/2;

% [W/m*K] Thermal conductivity of air.
ka4(p)=abs((4.9198e-011*Tf4(p)^3)-(1.608e-007*Tf4(p)^2)+(2.014e-004*Tf4(p))-0.020
796);

% [m^2/s] Kinematic viscosity of air.
nu4(p)=abs(((7.786e-005*Tf4(p)^2)+(4.4053e-002*Tf4(p))-2.4972)*1.0e-006);

% Prandtl #.
Pr4(p)=abs((-2.5065e-011*Tf4(p)^3)+(8.4944e-008*Tf4(p)^2)-(1.0417e-004*Tf4(p))+0.
74553);

% [K^-1] Exp. Coefficient of air.
B4(p)=1/Tf4(p);


% Emissivity of titanium.
E4(p)=abs((-5.0412e-008*T4(p)^2)+(2.4949e-004*T4(p))+0.051504);
E5(p)=abs((-5.0412e-008*T5(p)^2)+(2.4949e-004*T5(p))+0.051504);
```

```
% Solves for Rayleigh and Grashof #'s.
Gr4(p)=((g*B4(p)*(T4(p)-T5(p))*(Lc^3))/(nu4(p)^2));
Ra4(p)=Gr4(p)*Pr4(p);

if Ra4(p)==0
Ra4(p)=0.001;
else
Ra4(p)=Ra4(p);
end

% Nusselt correlation for circular annuli heated and cooled on the
% vertical curved surface.  Developed by de Vahl Davis and Thomas.
fpr4(p)=(1+((0.5/Pr4(p))^(9/16)))^(-16/9);
Nu4(p)=0.364*((Ra4(p)*fpr4(p))^0.25)*((r3/r2)^0.5);

% Solves for convective resistance using the average convection
% heat transfer coefficient within the annuli.
h4(p)=(Nu4(p)*ka4(p))/Lc;
Rco2(p)=(A4+A5)/(h4(p)*A4*A5);

% Calculates view factor.  Equation from the catalog of radiation
% configuration factors, interior of outer right circular cylinder
% of finite length to exterior of inner right circular coaxial
% cylinder [C-87].
R=r3/r2;
HH=Lc/r2;
F45=(1/R)*(1-((HH^2+R^2-1)/(4*HH))-1/pi*(acos((HH^2-R^2+1)/(HH^2+R^2-1))-(((sq
rt(((HH^2+R^2+1)^2)-(2*(R^2))))/(2*HH))*acos((HH^2-R^2+1)/(R*(HH^2+R^2-1))))-(
((HH^2-R^2+1)/(2*HH))*asin(1/R))));

% Solves the radiative resistance network for two surf enclosure,
% and linearizes the resistance to be used ICW the convective
% resistance.
Rr2(p)=((1-E4(p))/(E4(p)*A4))+(1/(A4*F45))+((1-E5(p))/(E5(p)*A5));
Rrad2(p)= 1/((sig/Rr2(p))*((T4(p)+T5(p))*(T4(p)^2+T5(p)^2)));

% Solves for total resistance.
Rt2(p)=((Rco2(p)*Rrad2(p))/(Rco2(p)+Rrad2(p)));

% Finite difference equation--explicit method.
T4(p+1)=2*(((H2(p)/Rc2(p))*(T3(p)-T4(p)))+((H2(p)/Rt2(p))*(T5(p)-T4(p)))+((T3(p)+
T4(p))/2))-T3(p+1);
```

```
if T4(p+1)<300
T4(p+1)=300;
else
T4(p+1)=T4(p+1);
end


%%% SOLVES SECTION 4 [T5] %%%

% [K] Film temperature to evaluate properties of titanium.
Tf5(p)=(T5(p)+T6(p))/2;

% [W/m*K] Thermal conductivity of canister wall.
kc5(p)=abs((1.7011e-008*Tf5(p)^3)-(4.3316e-005*Tf5(p)^2)+(2.7279e-002*Tf5(p))+20.
358);

% [J/kg*K] Specific Heat of canister wall.
cp5(p)=abs(((4.6480e-007)*Tf5(p)^3)-((1.4813e-003)*Tf5(p)^2)+(1.5387*Tf5(p))+139.9
3);

% [m^2/s]  Thermal diffusivity of canister wall.
alf5(p)=abs(((-4.532e-015)*Tf5(p)^3)+((1.7281e-011)*Tf5(p)^2)-(1.929e-008*Tf5(p))+1
.3594e-005);

% [kg/m^3] Density of canister wall.
rho5(p)=kc5(p)/(alf5(p)*cp5(p));

% Solves for the conductive resistance through the cylinder wall.
Rc3(p)=log(r2/r1)/(2*pi*kc5(p)*Lc);

% Finite difference equation--explicit method.
H3(p)=delt/(rho5(p)*cp5(p)*V3);
T5(p+1)=2*(((H3(p)/Rt2(p))*(T4(p)-T5(p)))+((H3(p)/Rc3(p))*(T6(p)-T5(p)))+((T5(p)+
T6(p))/2))-T6(p);


%%% SOLVES SECTION 5 [T6] %%%

% [K] Film temperature to evaluate air properties in 2nd annulus.
Tf6(p)=(T6(p)+T7(p))/2;
```

```
% [W/m*K] Thermal conductivity.
ka6(p)=abs((4.9198e-011*Tf6(p)^3)-(1.608e-007*Tf6(p)^2)+(2.014e-004*Tf6(p))-0.020
796);

% [m^2/s] Kinematic viscosity.
nu6(p)=abs(((7.786e-005*Tf6(p)^2)+(4.4053e-002*Tf6(p))-2.4972)*1.0e-006);

% Prandtl #.
Pr6(p)=abs((-2.5065e-011*Tf6(p)^3)+(8.4944e-008*Tf6(p)^2)-(1.0417e-004*Tf6(p))+0.
74553);

% [K^-1]  Exp. Coefficient of air.
B6(p)=1/Tf6(p);

% Emissivity of titanium.
E6(p)=abs((-5.0412e-008*T6(p)^2)+(2.4949e-004*T6(p))+0.051504);
E7(p)=abs((-5.0412e-008*T7(p)^2)+(2.4949e-004*T7(p))+0.051504);

% Solves for Rayleigh and Grashof #'s.
Gr5(p)=(g*B6(p)*(T6(p)-T7(p))*(Lc^3))/(nu6(p)^2);
Ra5(p)=Gr5(p)*Pr6(p);

if Ra5(p)==0
Ra5(p)=0.001;
else
Ra5(p)=Ra5(p);
end

% Nusselt correlation for circular annuli heated and cooled on the
% vertical curved surface.  Developed by de Vahl Davis and Thomas.
fpr5(p)=(1+((0.5/Pr6(p))^(9/16)))^(-16/9);
Nu5(p)=0.364*((Ra5(p)*fpr5(p))^0.25)*((r1/ro)^0.5);

% Solves for convective resistance using the average convection
% heat transfer coefficient within the annuli.
h5(p)=Nu5(p)*ka6(p)/Lc;
Rco3(p)=(A6+A7)/(h5(p)*A6*A7);

% Calculates view factor.  Equation from the catalog of radiation
% configuration factors, interior of outer right circular cylinder
% of finite length to exterior of inner right circular coaxial
% cylinder [C-87].
R1=r1/ro;
```

```
HH1=Lc/ro;
F67=(1/R1)*(1-((HH1^2+R1^2-1)/(4*HH1))-1/pi*(acos((HH1^2-R1^2+1)/(HH1^2+R1^
2-1))-(((sqrt(((HH1^2+R1^2+1)^2)-(2*(R1^2))))/(2*HH1))*acos((HH1^2-R1^2+1)/(R1*
(HH1^2+R1^2-1))))-(((HH1^2-R1^2+1)/(2*HH1))*asin(1/R1))));

% Solves the radiative resistance network for two surf enclosure,
% and linearizes the resistance to be used ICW the convective
% resistance.
Rr3(p)=((1-E6(p))/(E6(p)*A6))+(1/(A7*F67))+((1-E7(p))/(E7(p)*A7));
Rrad3(p)= 1/((sig/Rr3(p))*((T6(p)+T7(p))*(T6(p)^2+T7(p)^2)));

% Solves for total resistance.
Rt3(p)=(Rco3(p)*Rrad3(p))/(Rco3(p)+Rrad3(p));

% Finite difference equation--explicit method.
T6(p+1)=2*(((H3(p)/Rc3(p))*(T5(p)-T6(p)))+((H3(p)/Rt3(p))*(T7(p)-T6(p)))+((T5(p)+
T6(p))/2))-T5(p+1);

if T6(p+1)<300
T6(p+1)=300;
else
T6(p+1)=T6(p+1);
end

% [K] Film temperature to evaluate properties of aluminum.
Tf7(p)=(T7(p)+T8(p))/2;

% [W/m*K] Thermal conductivity of missile.
kc7(p)=237;

% [J/kg*K] Specific Heat of missile.
cp7(p)=903;

% [m^2/s]  Thermal diffusivity of missile.
alf7(p)=97.1e-006;

% [kg/m^3] Density of missile.
rho7(p)=2702;

% Solves for the conductive resistance through the cylinder wall.
Rc4(p)=log(ro/r)/(2*pi*kc7(p)*Lc);
```

```
% Finite difference equation--explicit method.
H4(p)=(delt/(rho7(p)*cp7(p)*V4));
T7(p+1)=2*(((H4(p)/Rt3(p))*(T6(p)-T7(p)))+((H4(p)/Rc4(p))*(T8(p)-T7(p)))+((T7(p)+
T8(p))/2))-T8(p);

T8(p+1)=2*(((H4(p)/Rc4(p))*(T7(p)-T8(p)))+((T7(p)+T8(p))/2))-T7(p+1);

if T8(p+1)<300
T8(p+1)=300;
else
T8(p+1)=T8(p+1);
end
end

t=t/60;
plot(t,T8); grid;
xlabel('Time (min)');
ylabel('Temperature (K)');
```

# APPENDIX B. CCL-FIRE PROGRAM CODE (2B-CENTER)

This MATLAB code solve for radiation resistance using the Taylor series expansion as described in the radiation section of Chapter II. This code is set up for the center CCL and scenario 2.

```
format bank
clear

% DIMENSIONS FOR CANISTERS & SURROUNDING VLS WALL.

w=1;              % [m] Width of for and aft bulkhead.
Lw=1;             % [m] Height of wall surrounding CCL module.
Lc=1;             % [m] Height of inner/outer canister wall.
Lm=1;             % [m] Length of missile.
delx=0.0048;      % [m] Thickness of wall surrounding CCL module.
r=0.00159;        % [m] Near center of missile (1/16 in).
ro=0.2586;        % [m] Radius of missile.
r1=0.2635;        % [m] Inside radius of inner cylinder wall.
r2=0.2667;        % [m] Outside radius of inner cylinder wall.
r3=0.3492;        % [m] Inside radius of outer cylinder wall.
r4=0.3571;        % [m] Outside radius of outer cylinder wall.
s=0.8382;         % [m] Distance between cylinder CL.
g=9.81;           % [m/s^2] Gravitational constant.
sig=5.67e-008;    % [W/m^2*K^4] Stefan-Boltzmann constant.
A1=w*Lw;          % [m^2]Area of VLS wall perp to dir of heat flux.
A2=A1;
A3=2*pi*r4*Lc;    % [m^2] Outer surface area of 1st cylinder.
A4=2*pi*r3*Lc;    % [m^2] Inner surface area of 1st cylinder.
A5=2*pi*r2*Lc;    % [m^2] Outer surface area of 2nd cylinder.
A6=2*pi*r1*Lc;    % [m^2] Inner surface area of 2nd cylinder.
A7=2*pi*ro*Lc;    % [m^2] Surface area of missile.
V1=delx*w*Lw;
V2=pi*Lc*(r4^2-r3^2);
V3=pi*Lc*(r2^2-r1^2);
V4=pi*ro^2*Lm;


% [K]  INITIAL AMBIENT CONDITIONS TO START ITERATION.

T2(1)=300;
```

```
T3(1)=300;
T4(1)=300;
T5(1)=300;
T6(1)=300;
T7(1)=300;
T8(1)=300;


% DEFINES TIME STEP AND NUMBER OF ITERATIONS

S=60000;      %      Number of iterations.
delt=0.36;    % [s]  Time step.

% BEGINS LOOP TO SOLVE FOR ALL TEMPS IN RESISTANCE NETWORK.

for p=1:S
p1=p

% [s] Time.
t(p)=(delt*(p-1));

dT(p)=t(p)*1.3333;
dTA(p)=t(p)*0.0128;
T1(p)=300+dT(p);
T1A(p)=1200+dTA(p);

if T1(p)<=1200
T1(p)=T1(p);
else
T1(p)=T1A(p);
end

t(p+1)=(delt*(p));
dT(p+1)=t(p+1)*1.3333;
dTA(p+1)=t(p+1)*0.0128;
T1(p+1)=300+dT(p+1);
T1A(p+1)=1200+dTA(p+1);

if T1(p+1)<=1200
T1(p+1)=T1(p+1);
else
T1(p+1)=T1A(p+1);
end
```

```
%%%  SOLVES SECTION 1 [T2] %%%

% [K] Film temperature to evaluate properties of mild steel
Tf1(p)=(T1(p)+T2(p))/2;

% [W/m*K] Thermal conductivity of bulkhead.
kw1(p)=abs((1.8869e-005*Tf1(p)^2)-(6.9896e-002*Tf1(p))+83.438);

% [J/kg*K] Specific Heat of bulkhead.
cp1(p)=abs(((-2.2828e-006)*Tf1(p)^3)+((4.6812e-003)*Tf1(p)^2)-(2.3469*Tf1(p))+800.99);

% [m^2/s] Thermal diffusivity of bulkhead.
alf1(p)=abs(((4.0118e-014)*Tf1(p)^3)-((7.9337e-011)*Tf1(p)^2)+(3.3733e-008*Tf1(p))+1.0388
e-005);

% [kg/m^3] Density of bulkhead.
rho1(p)=kw1(p)/(cp1(p)*alf1(p));

% Solves for the conductive resistance in bulkhead.
Rc1(p)=delx/(kw1(p)*A2);

% [K] Film temperature to evaluate properties in 1st air space.
Tf2(p)=(T2(p)+T3(p))/2;

% [W/m*K] Thermal conductivity of air.
ka2(p)=abs((4.9198e-011*Tf2(p)^3)-(1.608e-007*Tf2(p)^2)+(2.014e-004*Tf2(p))-0.020796);

% [m^2/s] Kinematic viscosity of air.
nu2(p)=abs(((7.786e-005*Tf2(p)^2)+(4.4053e-002*Tf2(p))-2.4972)*1.0e-006);

% Prandtl #.
Pr2(p)=abs((-2.5065e-011*Tf2(p)^3)+(8.4944e-008*Tf2(p)^2)-(1.0417e-004*Tf2(p))+0.74553);

% [K^-1] Exp. Coefficient of air .
B2(p)=1/Tf2(p);

% Emissivity of mild steel.
E2(p)=abs((-9.8416e-008*T2(p)^2)+(2.6912e-004*T2(p))+0.73699);

% Emissivity of titanium.
E3(p)=abs((-5.0412e-008*T3(p)^2)+(2.4949e-004*T3(p))+0.051504);
```

```
% Solves for Rayleigh and Grashof #'s WRT bulkhead inner surface.
Gr2(p)=((g*B2(p)*(T2(p)-Tf2(p))*(Lw^3))/(nu2(p)^2));
Ra2(p)=Gr2(p)*Pr2(p);

% Correlation to solve for the average Nusselt # over a
% vertical flat plat.  Recommended by Churchill and Chu, it is
% good over entire range of Rayleigh #'s.
Nu2(p)=(0.825+((0.387*(Ra2(p)^(1/6)))/((1+((0.492/Pr2(p))^(9/16)))^(8/27))))^2;

% Solves for convective resistance using the average convection
% heat transfer coefficient over the bulkhead inner surface.
h2(p)=Nu2(p)*ka2(p)/Lw;
Rco1a(p)=1/(h2(p)*A2);

% Solves for Rayleigh and Grashof #'s WRT cylinder outer surface.
Gr3(p)=(g*B2(p)*(Tf2(p)-T3(p))*(Lc^3))/(nu2(p)^2);
Ra3(p)=Gr3(p)*Pr2(p);

% IF-THEN LOOP TO DETERMINE IF THE OUTER WALL OF THE CYLINDER
% CAN BE APPROXIMATED AS A PLANE WALL. IF A PLANE WALL CHURCHILL
% AND CHU'S CORRELATION FOR A VERTICAL SURFACE IS USED.  IF
% THERE ARE APPRECIABLE CURVATURE EFFECTS A CORRELATION DEVELOPED
% BY LE FEVRE AND EDE BASED ON CYLINDER HEIGHT.

if Gr3(p)==0
Nu3(p)=((4/3)*((7*Gr3(p)*Pr2(p)^2)/(5*(20+21*Pr2(p))))^0.25)+((4*Lc*(272+315*Pr2(p)))/(3
5*2*r4*(64+63*Pr2(p))));
else
if ((2*r4)/Lc)>=35/(Gr3(p)^1/4)
Nu3(p)=(0.825+((0.387*(Ra3(p)^(1/6)))/((1+((0.492/Pr2(p))^(9/16)))^(8/27))))^2;
else
Nu3(p)=((4/3)*((7*Gr3(p)*Pr2(p)^2)/(5*(20+21*Pr2(p))))^0.25)+((4*Lc*(272+315*Pr(p)))/(35
*2*r4*(64+63*Pr2(p))));
end
end

% Solves for convective resistance using the average convection
% heat transfer coefficient over outer surface of the cylinder.
h3(p)=(Nu3(p)*ka2(p))/Lc;
Rco1b(p)=1/(h3(p)*A3);

% Adds convective resistances in series.
Rco1(p)=Rco1a(p)+Rco1b(p);
```

```
% Calculates view factor.  Equation from the catalog of radiation
% configuration factors, infinite plane to a row of pipes [C-6].
D=(2*r4)/s;
F23=1-((1-D^2)^0.5)+(D*atan(((1-D^2)/D^2)^0.5));

% Solves the radiative resistance network for two surf enclosure,
% and linearizes the resistance to be used ICW the convective
% resistance.
Rr1(p)=((1-E2(p))/(E2(p)*A2))+(1/(A2*F23))+((1-E3(p))/(E3(p)*A3));
qo1(p)=(sig*(T2(p)^4-T3(p)^4))/Rr1(p);

if qo1(p)==0
Rrad1(p)=Rr1(p)/(4*sig*T3(p)^3);
else
Rrad1(p)=1/((qo1(p)/(T2(p)-T3(p)))+((4*sig*T3(p)^3)/Rr1(p)));
end

% Solves for total resistance, [T3], and begins next iteration.
Rt(p)=(Rco1(p)*Rrad1(p))/(Rrad1(p)+Rco1(p));

% Finite difference equation--explicit method.
H1(p)=delt/(rho1(p)*cp1(p)*V1);
T2(p+1)=2*(((H1(p)/Rc1(p))*(T1(p)-T2(p)))+((H1(p)/Rt(p))*(T3(p)-T2(p)))+((T2(p)+T1(p))/2)
)-T1(p+1);

if T2(p+1)<300
T2(p+1)=300;
else
T2(p+1)=T2(p+1);
end


%%% SOLVES SECTION 2 [T3] %%%

% [K] Film temperature to evaluate properties of titanium.
Tf3(p)=(T3(p)+T4(p))/2;

% [W/m*K] Thermal conductivity of canister wall.
kc3(p)=abs((1.7011e-008*Tf3(p)^3)-(4.3316e-005*Tf3(p)^2)+(2.7279e-002*Tf3(p))+20.358);

% [J/kg*K] Specific Heat of canister wall.
cp3(p)=abs(((4.6480e-007)*Tf3(p)^3)-((1.4813e-003)*Tf3(p)^2)+(1.5387*Tf3(p))+139.93);
```

```
% [m^2/s]  Thermal diffusivity of canister wall.
alf3(p)=abs(((-4.532e-015)*Tf3(p)^3)+((1.7281e-011)*Tf3(p)^2)-(1.929e-008*Tf3(p))+1.3594e-
005);

% [kg/m^3] Density of canister wall.
rho3(p)=kc3(p)/(alf3(p)*cp3(p));

% Solves for the conductive resistance through the cylinder wall.
Rc2(p)=log(r4/r3)/(2*pi*kc3(p)*Lc);

% Finite difference equation--explicit method.
H2(p)=delt/(rho3(p)*cp3(p)*V2);
T3(p+1)=2*(((H2(p)/Rt(p))*(T2(p)-T3(p)))+((H2(p)/Rc2(p))*(T4(p)-T3(p)))+((T3(p)+T4(p))/2)
)-T4(p);


%%% SOLVES SECTION 3 [T4] %%%

% [K] Film temperature to evaluate air properties in 1st annulus.
Tf4(p)=(T4(p)+T5(p))/2;

% [W/m*K] Thermal conductivity of air.
ka4(p)=abs((4.9198e-011*Tf4(p)^3)-(1.608e-007*Tf4(p)^2)+(2.014e-004*Tf4(p))-0.020796);

% [m^2/s] Kinematic viscosity of air.
nu4(p)=abs(((7.786e-005*Tf4(p)^2)+(4.4053e-002*Tf4(p))-2.4972)*1.0e-006);

% Prandtl #.
Pr4(p)=abs((-2.5065e-011*Tf4(p)^3)+(8.4944e-008*Tf4(p)^2)-(1.0417e-004*Tf4(p))+0.74553);

% [K^-1] Exp. Coefficient of air.
B4(p)=1/Tf4(p);

% Emissivity of titanium.
E4(p)=abs((-5.0412e-008*T4(p)^2)+(2.4949e-004*T4(p))+0.051504);
E5(p)=abs((-5.0412e-008*T5(p)^2)+(2.4949e-004*T5(p))+0.051504);

% Solves for Rayleigh and Grashof #'s.
Gr4(p)=((g*B4(p)*(T4(p)-T5(p))*(Lc^3))/(nu4(p)^2));
Ra4(p)=Gr4(p)*Pr4(p);
```

```
if Ra4(p)==0
Ra4(p)=0.001;
else
Ra4(p)=Ra4(p);
end

% Nusselt correlation for curcular annuli heated and cooled on the
% vertical curved surface.  Developed by de Vahl Davis and Thomas.
fpr4(p)=(1+((0.5/Pr4(p))^(9/16)))^(-16/9);
Nu4(p)=0.364*((Ra4(p)*fpr4(p))^0.25)*((r3/r2)^0.5);

% Solves for convective resistance using the average convection
% heat transfer coefficient within the annuli.
h4(p)=(Nu4(p)*ka4(p))/Lc;
Rco2(p)=(A4+A5)/(h4(p)*A4*A5);

% Calculates view factor.  Equation from the catalog of radiation
% configuration factors, interior of outer right circular cylinder
% of finite length to exterior of inner right circular coaxial
% cylinder [C-87].
R=r3/r2;
HH=Lc/r2;
F45=(1/R)*(1-((HH^2+R^2-1)/(4*HH))-1/pi*(acos((HH^2-R^2+1)/(HH^2+R^2-1))-(((sqrt(((H
H^2+R^2+1)^2)-(2*(R^2))))/(2*HH))*acos((HH^2-R^2+1)/(R*(HH^2+R^2-1))))-(((HH^2-R^2
+1)/(2*HH))*asin(1/R))));

% Solves the radiative resistance network for two surf enclosure,
% and linearizes the resistance to be used ICW the convective
% resistance.
Rr2(p)=((1-E4(p))/(E4(p)*A4))+(1/(A4*F45))+((1-E5(p))/(E5(p)*A5));
qo2(p)=(sig*(T4(p)^4-T5(p)^4))/Rr2(p);

if qo2(p)==0
Rrad2(p)=Rr2(p)/(4*sig*T5(p)^3);
else
Rrad2(p)=1/((qo2(p)/(T4(p)-T5(p)))+((4*sig*T5(p)^3)/Rr2(p)));
end

% Solves for total resistance.
Rt2(p)=((Rco2(p)*Rrad2(p))/(Rco2(p)+Rrad2(p)));
```

```
% Finite difference equation--explicit method.
T4(p+1)=2*(((H2(p)/Rc2(p))*(T3(p)-T4(p)))+((H2(p)/Rt2(p))*(T5(p)-T4(p)))+((T3(p)+T4(p))/
2))-T3(p+1);

if T4(p+1)<300
T4(p+1)=300;
else
T4(p+1)=T4(p+1);
end


%%% SOLVES SECTION 4 [T5] %%%

% [K] Film temperature to evaluate properties of titanium.
Tf5(p)=(T5(p)+T6(p))/2;

% [W/m*K] Thermal conductivity of canister wall.
kc5(p)=abs((1.7011e-008*Tf5(p)^3)-(4.3316e-005*Tf5(p)^2)+(2.7279e-002*Tf5(p))+20.358);

% [J/kg*K] Specific Heat of canister wall.
cp5(p)=abs(((4.6480e-007)*Tf5(p)^3)-((1.4813e-003)*Tf5(p)^2)+(1.5387*Tf5(p))+139.93);

% [m^2/s]  Thermal diffusivity of canister wall.
alf5(p)=abs(((-4.532e-015)*Tf5(p)^3)+((1.7281e-011)*Tf5(p)^2)-(1.929e-008*Tf5(p))+1.3594e-
005);

% [kg/m^3] Density of canister wall.
rho5(p)=kc5(p)/(alf5(p)*cp5(p));

% Solves for the conductive resistance through the cylinder wall.
Rc3(p)=log(r2/r1)/(2*pi*kc5(p)*Lc);

% Finite difference equation--explicit method.
H3(p)=delt/(rho5(p)*cp5(p)*V3);
T5(p+1)=2*(((H3(p)/Rt2(p))*(T4(p)-T5(p)))+((H3(p)/Rc3(p))*(T6(p)-T5(p)))+((T5(p)+T6(p))/
2))-T6(p);


%%% SOLVES SECTION 5 [T6] %%%

% [K] Film temperature to evaluate air properties in 2nd annulus.
Tf6(p)=(T6(p)+T7(p))/2;
```

```
% [W/m*K] Thermal conductivity.
ka6(p)=abs((4.9198e-011*Tf6(p)^3)-(1.608e-007*Tf6(p)^2)+(2.014e-004*Tf6(p))-0.020796);

% [m^2/s] Kinematic viscosity.
nu6(p)=abs(((7.786e-005*Tf6(p)^2)+(4.4053e-002*Tf6(p))-2.4972)*1.0e-006);

% Prandtl #.
Pr6(p)=abs((-2.5065e-011*Tf6(p)^3)+(8.4944e-008*Tf6(p)^2)-(1.0417e-004*Tf6(p))+0.74553);

% [K^-1]  Exp. Coefficient of air.
B6(p)=1/Tf6(p);

% Emissivity of titanium.
E6(p)=abs((-5.0412e-008*T6(p)^2)+(2.4949e-004*T6(p))+0.051504);
E7(p)=abs((-5.0412e-008*T7(p)^2)+(2.4949e-004*T7(p))+0.051504);

% Solves for Rayleigh and Grashof #'s.
Gr5(p)=(g*B6(p)*(T6(p)-T7(p))*(Lc^3))/(nu6(p)^2);
Ra5(p)=Gr5(p)*Pr6(p);

if Ra5(p)==0
Ra5(p)=0.001;
else
Ra5(p)=Ra5(p);
end

% Nusselt correlation for curcular annuli heated and cooled on the
% vertical curved surface.  Developed by de Vahl Davis and Thomas.
fpr5(p)=(1+((0.5/Pr6(p))^(9/16)))^(-16/9);
Nu5(p)=0.364*((Ra5(p)*fpr5(p))^0.25)*((r1/ro)^0.5);

% Solves for convective resistance using the average convection
% heat transfer coefficient within the annuli.
h5(p)=Nu5(p)*ka6(p)/Lc;
Rco3(p)=(A6+A7)/(h5(p)*A6*A7);

% Calculates view factor.  Equation from the catalog of radiation
% configuration factors, interior of outer right circular cylinder
% of finite length to exterior of inner right circular coaxial
% cylinder [C-87].
R1=r1/ro;
HH1=Lc/ro;
```

```
F67=(1/R1)*(1-((HH1^2+R1^2-1)/(4*HH1))-1/pi*(acos((HH1^2-R1^2+1)/(HH1^2+R1^2-1))-((
(sqrt(((HH1^2+R1^2+1)^2)-(2*(R1^2))))/(2*HH1))*acos((HH1^2-R1^2+1)/(R1*(HH1^2+R1^2
-1))))-(((HH1^2-R1^2+1)/(2*HH1))*asin(1/R1))));

% Solves the radiative resistance network for two surf enclosure,
% and linearizes the resistance to be used ICW the convective
% resistance.
Rr3(p)=((1-E6(p))/(E6(p)*A6))+(1/(A7*F67))+((1-E7(p))/(E7(p)*A7));
qo3(p)=(sig*(T6(p)^4-T7(p)^4))/Rr3(p);

if qo3(p)==0
Rrad3(p)=Rr3(p)/(4*sig*T7(p)^3);
else
Rrad3(p)=1/((qo3(p)/(T6(p)-T7(p)))+((4*sig*T7(p)^3)/Rr3(p)));
end

% Solves for total resistance.
Rt3(p)=(Rco3(p)*Rrad3(p))/(Rco3(p)+Rrad3(p));

% Finite difference equation--explicit method.
T6(p+1)=2*(((H3(p)/Rc3(p))*(T5(p)-T6(p)))+((H3(p)/Rt3(p))*(T7(p)-T6(p)))+((T5(p)+T6(p))/
2))-T5(p+1);

if T6(p+1)<300
T6(p+1)=300;
else
T6(p+1)=T6(p+1);
end

% [K] Film temperature to evaluate properties of aluminum.
Tf7(p)=(T7(p)+T8(p))/2;

% [W/m*K] Thermal conductivity of missile.
kc7(p)=237;

% [J/kg*K] Specific Heat of missile.
cp7(p)=903;

% [m^2/s]  Thermal diffusivity of missile.
alf7(p)=97.1e-006;

% [kg/m^3] Density of missile.
rho7(p)=2702;
```

```
% Solves for the conductive resistance through the cylinder wall.
Rc4(p)=log(ro/r)/(2*pi*kc7(p)*Lc);

% Finite difference equation--explicit method.
H4(p)=(delt/(rho7(p)*cp7(p)*V4));
T7(p+1)=2*(((H4(p)/Rt3(p))*(T6(p)-T7(p)))+((H4(p)/Rc4(p))*(T8(p)-T7(p)))+((T7(p)+T8(p))/
2))-T8(p);

T8(p+1)=2*(((H4(p)/Rc4(p))*(T7(p)-T8(p)))+((T7(p)+T8(p))/2))-T7(p+1);

if T8(p+1)<300
T8(p+1)=300;
else
T8(p+1)=T8(p+1);
end
end
t=t/60;

plot(t,T8); grid;
xlabel('Time (min)');
ylabel('Temperature (K)');
```

# APPENDIX C. CCL-FIRE PROGRAM CODE (2A-CORNER)

This MATLAB code solves for the radiation resistance explicitly as described in the radiation section of Chapter II. This code is set up for scenario 2 and the corner CCL in which the adjoining bulkhead is assumed to be a reradiating surface.

```
format bank
clear

% DIMENSIONS FOR CANISTERS & SURROUNDING VLS WALL.

w=1;            % [m] Width of for and aft bulkhead.
w1=1;           % [m] Width of port and stbd bulkhead.
Lw=1;           % [m] Height of wall surrounding CCL module.
Lc=1;           % [m] Height of inner/outer canister wall.
Lm=1;           % [m] Length of missile.
delx=0.0048;    % [m] Thickness of wall surrounding CCL module.
r=0.00159;      % [m] Near center of missile (1/16 in).
ro=0.2586;      % [m] Radius of missile.
r1=0.2635;      % [m] Inside radius of inner cylinder wall.
r2=0.2667;      % [m] Outside radius of inner cylinder wall.
r3=0.3492;      % [m] Inside radius of outer cylinder wall.
r4=0.3571;      % [m] Outside radius of outer cylinder wall.
s=0.8382;       % [m] Distance between cylinder CL.
g=9.81;         % [m/s^2] Gravitational constant.
sig=5.67e-008;  % [W/m^2*K^4] Stefan-Boltzman constant.
AR=w1*Lw;       % [m^2] Area of reradiative bulkhead
A2=w*Lw;        % [m^2] Area of VLS wall perp to dir of heat flux.
A3=2*pi*r4*Lc;  % [m^2] Outer surface area of 1st cylinder.
A4=2*pi*r3*Lc;  % [m^2] Inner surface area of 1st cylinder.
A5=2*pi*r2*Lc;  % [m^2] Outer surface area of 2nd cylinder.
A6=2*pi*r1*Lc;  % [m^2] Inner surface area of 2nd cylinder.
A7=2*pi*ro*Lc;  % [m^2] Surface area of missile.
V1=delx*w*Lw;
V2=pi*Lc*(r4^2-r3^2);
V3=pi*Lc*(r2^2-r1^2);
V4=pi*ro^2*Lm;
```

```
% [K]  INITIAL AMBIENT CONDITIONS TO START ITERATION.

T2(1)=300;
T3(1)=300;
T4(1)=300;
T5(1)=300;
T6(1)=300;
T7(1)=300;
T8(1)=300;

% DEFINES TIME STEP AND NUMBER OF ITERATIONS

S=45000;      %      Number of iterations.
delt=0.36;    %  [s] Time step.


% BEGINS LOOP TO SOLVE FOR ALL TEMPS IN RESISTANCE NETWORK.

for p=1:S
p1=p

% [s] Time.
t(p)=(delt*(p-1));

% Temperature rise from ambient to 1325 K over a 5 minute period.
% This temp is then maintained for the duration of the fire.
dT(p)=t(p)*1.3333;
dTA(p)=t(p)*0.0128;
T1(p)=300+dT(p);
T1A(p)=1200+dTA(p);

if T1(p)<=1200
T1(p)=T1(p);
else
T1(p)=T1A(p);
end

t(p+1)=(delt*(p));
dT(p+1)=t(p+1)*1.3333;
dTA(p+1)=t(p+1)*0.0128;
T1(p+1)=300+dT(p+1);
T1A(p+1)=1200+dTA(p+1);
```

```
if T1(p+1)<=1200
T1(p+1)=T1(p+1);
else
T1(p+1)=T1A(p+1);
end


%%%  SOLVES SECTION 1 [T2] %%%

% [K] Film temperature to evaluate properties of mild steel
Tf1(p)=(T1(p)+T2(p))/2;

% [W/m*K] Thermal conductivity of bulkhead.
kw1(p)=abs((1.8869e-005*Tf1(p)^2)-(6.9896e-002*Tf1(p))+83.438);

% [J/kg*K] Specific Heat of bulkhead.
cp1(p)=abs(((-2.2828e-006)*Tf1(p)^3)+((4.6812e-003)*Tf1(p)^2)-(2.3469*Tf1(p))+800.
99);

% [m^2/s] Thermal diffusivity of bulkhead.
alf1(p)=abs(((4.0118e-014)*Tf1(p)^3)-((7.9337e-011)*Tf1(p)^2)+(3.3733e-008*Tf1(p))
+1.0388e-005);

% [kg/m^3] Density of bulkhead.
rho1(p)=kw1(p)/(cp1(p)*alf1(p));

% Solves for the conductive resistance in bulkhead.
Rc1(p)=delx/(kw1(p)*A2);

% [K] Film temperature to evaluate properties in 1st air space.
Tf2(p)=(T2(p)+T3(p))/2;

% [W/m*K] Thermal conductivity of air.
ka2(p)=abs((4.9198e-011*Tf2(p)^3)-(1.608e-007*Tf2(p)^2)+(2.014e-004*Tf2(p))-0.020
796);

% [m^2/s] Kinematic viscosity of air.
nu2(p)=abs(((7.786e-005*Tf2(p)^2)+(4.4053e-002*Tf2(p))-2.4972)*1.0e-006);

% Prandtl #.
Pr2(p)=abs((-2.5065e-011*Tf2(p)^3)+(8.4944e-008*Tf2(p)^2)-(1.0417e-004*Tf2(p))+0.
74553);
```

```
% [K^-1] Exp. Coefficient of air .
B2(p)=1/Tf2(p);

% Emissivity of mild steel.
E2(p)=abs((-9.8416e-008*T2(p)^2)+(2.6912e-004*T2(p))+0.73699);

% Emissivity of titanium.
E3(p)=abs((-5.0412e-008*T3(p)^2)+(2.4949e-004*T3(p))+0.051504);

% Solves for Rayleigh and Grashof #'s WRT bulkhead inner surface.
Gr2(p)=((g*B2(p)*(T2(p)-Tf2(p))*(Lw^3))/(nu2(p)^2));
Ra2(p)=Gr2(p)*Pr2(p);

% Correlation to solve for the average Nusselt # over a
% vertical flat plat.  Recommended by Churchill and Chu, it is
% good over entire range of Rayleigh #'s.
Nu2(p)=(0.825+((0.387*(Ra2(p)^(1/6)))/((1+((0.492/Pr2(p))^(9/16)))^(8/27))))^2;

% Solves for convective resistance using the average convection
% heat transfer coefficient over the bulkhead inner surface.
h2(p)=Nu2(p)*ka2(p)/Lw;
Rco1a(p)=1/(h2(p)*A2);

% Solves for Rayleigh and Grashof #'s WRT cylinder outer surface.
Gr3(p)=(g*B2(p)*(Tf2(p)-T3(p))*(Lc^3))/(nu2(p)^2);
Ra3(p)=Gr3(p)*Pr2(p);

% IF-THEN LOOP TO DETERMINE IF THE OUTER WALL OF THE CYLINDER
% CAN BE APPROXIMATED AS A PLANE WALL. IF A PLANE WALL
% CHURCHILL
% AND CHU'S CORRELATION FOR A VERTICAL SURFACE IS USED.  IF
% THERE ARE APPRECIABLE CURVATURE EFFECTS A CORRELATION
% DEVELOPED
% BY LE FEVRE AND EDE BASED ON CYLINDER HEIGHT.

if Gr3(p)==0
Nu3(p)=((4/3)*((7*Gr3(p)*Pr2(p)^2)/(5*(20+21*Pr2(p))))^0.25)+((4*Lc*(272+315*Pr2
(p)))/(35*2*r4*(64+63*Pr2(p))));
else
if ((2*r4)/Lc)>=35/(Gr3(p)^1/4)
Nu3(p)=(0.825+((0.387*(Ra3(p)^(1/6)))/((1+((0.492/Pr2(p))^(9/16)))^(8/27))))^2;
else
```

```
Nu3(p)=((4/3)*((7*Gr3(p)*Pr2(p)^2)/(5*(20+21*Pr2(p))))^0.25)+((4*Lc*(272+315*Pr2
(p)))/(35*2*r4*(64+63*Pr2(p))));
end
end

% Solves for convective resistance using the average convection
% heat transfer coefficient over outer surface of the cylinder.
h3(p)=(Nu3(p)*ka2(p))/Lc;
Rco1b(p)=1/(h3(p)*A3);

% Adds convective resistances in series.
Rco1(p)=Rco1a(p)+Rco1b(p);

% Calculates view factor.  Equation from the catalog of radiation
% configuration factors, infinite plane to a row of pipes [C-6].
D=(2*r4)/s;
F23=1-((1-D^2)^0.5)+(D*atan(((1-D^2)/D^2)^0.5));
FR3=F23;
F2R=0.5*(1+(w1/w)-sqrt(1+((w1/w)^2)));

% Solves the radiative resistance network for two surf enclosure,
% and linearizes the resistance to be used ICW the convective
% resistance.
J1=1/(A2*F2R);
J2=1/(AR*FR3);
JT=(J1+J2)^(-1);
Rr1(p)=((1-E2(p))/(E2(p)*A2))+(1/((A2*F23)+JT))+((1-E3(p))/(E3(p)*A3));
Rrad1(p)= 1/((sig/Rr1(p))*((T2(p)+T3(p))*(T2(p)^2+T3(p)^2)));

% Solves for total resistance, [T3], and begins next iteration.
Rt(p)=(Rco1(p)*Rrad1(p))/(Rrad1(p)+Rco1(p));

% Finite difference equation--explicit method.
H1(p)=delt/(rho1(p)*cp1(p)*V1);
T2(p+1)=2*(((H1(p)/Rc1(p))*(T1(p)-T2(p)))+((H1(p)/Rt(p))*(T3(p)-T2(p)))+((T2(p)+T
1(p))/2))-T1(p+1);

if T2(p+1)<300
T2(p+1)=300;
else
T2(p+1)=T2(p+1);
end
```

```
%%% SOLVES SECTION 2 [T3] %%%

% [K] Film temperature to evaluate properties of titanium.
Tf3(p)=(T3(p)+T4(p))/2;

% [W/m*K] Thermal conductivity of canister wall.
kc3(p)=abs((1.7011e-008*Tf3(p)^3)-(4.3316e-005*Tf3(p)^2)+(2.7279e-002*Tf3(p))+20.
358);

% [J/kg*K] Specific Heat of canister wall.
cp3(p)=abs(((4.6480e-007)*Tf3(p)^3)-((1.4813e-003)*Tf3(p)^2)+(1.5387*Tf3(p))+139.9
3);

% [m^2/s]  Thermal diffusivity of canister wall.
alf3(p)=abs(((-4.532e-015)*Tf3(p)^3)+((1.7281e-011)*Tf3(p)^2)-(1.929e-008*Tf3(p))+1
.3594e-005);

% [kg/m^3] Density of canister wall.
rho3(p)=kc3(p)/(alf3(p)*cp3(p));

% Solves for the conductive resistance through the cylinder wall.
Rc2(p)=log(r4/r3)/(2*pi*kc3(p)*Lc);

% Finite difference equation--explicit method.
H2(p)=delt/(rho3(p)*cp3(p)*V2);
T3(p+1)=2*(((H2(p)/Rt(p))*(T2(p)-T3(p)))+((H2(p)/Rc2(p))*(T4(p)-T3(p)))+((T3(p)+T
4(p))/2))-T4(p);


%%% SOLVES SECTION 3 [T4] %%%

% [K] Film temperature to evaluate air properties in 1st annulus.
Tf4(p)=(T4(p)+T5(p))/2;

% [W/m*K] Thermal conductivity of air.
ka4(p)=abs((4.9198e-011*Tf4(p)^3)-(1.608e-007*Tf4(p)^2)+(2.014e-004*Tf4(p))-0.020
796);

% [m^2/s] Kinematic viscosity of air.
nu4(p)=abs(((7.786e-005*Tf4(p)^2)+(4.4053e-002*Tf4(p))-2.4972)*1.0e-006);
```

```
% Prandtl #.
Pr4(p)=abs((-2.5065e-011*Tf4(p)^3)+(8.4944e-008*Tf4(p)^2)-(1.0417e-004*Tf4(p))+0.
74553);

% [K^-1] Exp. Coefficient of air.
B4(p)=1/Tf4(p);

% Emissivity of titanium.
E4(p)=abs((-5.0412e-008*T4(p)^2)+(2.4949e-004*T4(p))+0.051504);
E5(p)=abs((-5.0412e-008*T5(p)^2)+(2.4949e-004*T5(p))+0.051504);

% Solves for Rayleigh and Grashof #'s.
Gr4(p)=((g*B4(p)*(T4(p)-T5(p))*(Lc^3))/(nu4(p)^2));
Ra4(p)=Gr4(p)*Pr4(p);

if Ra4(p)==0
Ra4(p)=0.001;
else
Ra4(p)=Ra4(p);
end

% Nusselt correlation for circular annuli heated and cooled on the
% vertical curved surface.  Developed by de Vahl Davis and Thomas.
fpr4(p)=(1+((0.5/Pr4(p))^(9/16)))^(-16/9);
Nu4(p)=0.364*((Ra4(p)*fpr4(p))^0.25)*((r3/r2)^0.5);

% Solves for convective resistance using the average convection
% heat transfer coefficient within the annuli.
h4(p)=(Nu4(p)*ka4(p))/Lc;
Rco2(p)=(A4+A5)/(h4(p)*A4*A5);

% Calculates view factor.  Equation from the catalog of radiation
% configuration factors, interior of outer right circular cylinder
% of finite length to exterior of inner right circular coaxial
% cylinder [C-87].
R=r3/r2;
HH=Lc/r2;
F45=(1/R)*(1-((HH^2+R^2-1)/(4*HH))-1/pi*(acos((HH^2-R^2+1)/(HH^2+R^2-1))-(((sq
rt(((HH^2+R^2+1)^2)-(2*(R^2))))/(2*HH))*acos((HH^2-R^2+1)/(R*(HH^2+R^2-1))))-(
((HH^2-R^2+1)/(2*HH))*asin(1/R))));
```

```
% Solves the radiative resistance network for two surf enclosure,
% and linearizes the resistance to be used ICW the convective
% resistance.
Rr2(p)=((1-E4(p))/(E4(p)*A4))+(1/(A4*F45))+((1-E5(p))/(E5(p)*A5));
Rrad2(p)= 1/((sig/Rr2(p))*((T4(p)+T5(p))*(T4(p)^2+T5(p)^2)));

% Solves for total resistance.
Rt2(p)=((Rco2(p)*Rrad2(p))/(Rco2(p)+Rrad2(p)));

% Finite difference equation--explicit method.
T4(p+1)=2*(((H2(p)/Rc2(p))*(T3(p)-T4(p)))+((H2(p)/Rt2(p))*(T5(p)-T4(p)))+((T3(p)+
T4(p))/2))-T3(p+1);

if T4(p+1)<300
T4(p+1)=300;
else
T4(p+1)=T4(p+1);
end


%%% SOLVES SECTION 4 [T5] %%%

% [K] Film temperature to evaluate properties of titanium.
Tf5(p)=(T5(p)+T6(p))/2;

% [W/m*K] Thermal conductivity of canister wall.
kc5(p)=abs((1.7011e-008*Tf5(p)^3)-(4.3316e-005*Tf5(p)^2)+(2.7279e-002*Tf5(p))+20.
358);

% [J/kg*K] Specific Heat of canister wall.
cp5(p)=abs(((4.6480e-007)*Tf5(p)^3)-((1.4813e-003)*Tf5(p)^2)+(1.5387*Tf5(p))+139.9
3);

% [m^2/s]  Thermal diffusivity of canister wall.
alf5(p)=abs(((-4.532e-015)*Tf5(p)^3)+((1.7281e-011)*Tf5(p)^2)-(1.929e-008*Tf5(p))+1
.3594e-005);

% [kg/m^3] Density of canister wall.
rho5(p)=kc5(p)/(alf5(p)*cp5(p));

% Solves for the conductive resistance through the cylinder wall.
Rc3(p)=log(r2/r1)/(2*pi*kc5(p)*Lc);
```

```
% Finite difference equation--explicit method.
H3(p)=delt/(rho5(p)*cp5(p)*V3);
T5(p+1)=2*(((H3(p)/Rt2(p))*(T4(p)-T5(p)))+((H3(p)/Rc3(p))*(T6(p)-T5(p)))+((T5(p)+
T6(p))/2))-T6(p);


%%% SOLVES SECTION 5 [T6] %%%

% [K] Film temperature to evaluate air properties in 2nd annulus.
Tf6(p)=(T6(p)+T7(p))/2;

% [W/m*K] Thermal conductivity.
ka6(p)=abs((4.9198e-011*Tf6(p)^3)-(1.608e-007*Tf6(p)^2)+(2.014e-004*Tf6(p))-0.020
796);

% [m^2/s] Kinematic viscosity.
nu6(p)=abs(((7.786e-005*Tf6(p)^2)+(4.4053e-002*Tf6(p))-2.4972)*1.0e-006);

% Prandtl #.
Pr6(p)=abs((-2.5065e-011*Tf6(p)^3)+(8.4944e-008*Tf6(p)^2)-(1.0417e-004*Tf6(p))+0.
74553);

% [K^-1]  Exp. Coefficient of air.
B6(p)=1/Tf6(p);

% Emissivity of titanium.
E6(p)=abs((-5.0412e-008*T6(p)^2)+(2.4949e-004*T6(p))+0.051504);
E7(p)=abs((-5.0412e-008*T7(p)^2)+(2.4949e-004*T7(p))+0.051504);

% Solves for Rayleigh and Grashof #'s.
Gr5(p)=(g*B6(p)*(T6(p)-T7(p))*(Lc^3))/(nu6(p)^2);
Ra5(p)=Gr5(p)*Pr6(p);

if Ra5(p)==0
Ra5(p)=0.001;
else
Ra5(p)=Ra5(p);
end

% Nusselt correlation for circular annuli heated and cooled on the
% vertical curved surface.  Developed by de Vahl Davis and Thomas.
fpr5(p)=(1+((0.5/Pr6(p))^(9/16)))^(-16/9);
Nu5(p)=0.364*((Ra5(p)*fpr5(p))^0.25)*((r1/ro)^0.5);
```

```
% Solves for convective resistance using the average convection
% heat transfer coefficient within the annuli.
h5(p)=Nu5(p)*ka6(p)/Lc;
Rco3(p)=(A6+A7)/(h5(p)*A6*A7);

% Calculates view factor.  Equation from the catalog of radiation
% configuration factors, interior of outer right circular cylinder
% of finite length to exterior of inner right circular coaxial
% cylinder [C-87].
R1=r1/ro;
HH1=Lc/ro;
F67=(1/R1)*(1-((HH1^2+R1^2-1)/(4*HH1))-1/pi*(acos((HH1^2-R1^2+1)/(HH1^2+R1^
2-1))-(((sqrt(((HH1^2+R1^2+1)^2)-(2*(R1^2))))/(2*HH1))*acos((HH1^2-R1^2+1)/(R1*
(HH1^2+R1^2-1))))-(((HH1^2-R1^2+1)/(2*HH1))*asin(1/R1))));

% Solves the radiative resistance network for two surf enclosure,
% and linearizes the resistance to be used ICW the convective
% resistance.
Rr3(p)=((1-E6(p))/(E6(p)*A6))+(1/(A7*F67))+((1-E7(p))/(E7(p)*A7));
Rrad3(p)= 1/((sig/Rr3(p))*((T6(p)+T7(p))*(T6(p)^2+T7(p)^2)));

% Solves for total resistance.
Rt3(p)=(Rco3(p)*Rrad3(p))/(Rco3(p)+Rrad3(p));

% Finite difference equation--explicit method.
T6(p+1)=2*(((H3(p)/Rc3(p))*(T5(p)-T6(p)))+((H3(p)/Rt3(p))*(T7(p)-T6(p)))+((T5(p)+
T6(p))/2))-T5(p+1);

if T6(p+1)<300
T6(p+1)=300;
else
T6(p+1)=T6(p+1);
end

% [K] Film temperature to evaluate properties of aluminum.
Tf7(p)=(T7(p)+T8(p))/2;

% [W/m*K] Thermal conductivity of missile.
kc7(p)=237;

% [J/kg*K] Specific Heat of missile.
cp7(p)=903;
```

```
% [m^2/s]  Thermal diffusivity of missile.
alf7(p)=97.1e-006;

% [kg/m^3] Density of missile.
rho7(p)=2702;

% Solves for the conductive resistance through the cylinder wall.
Rc4(p)=log(ro/r)/(2*pi*kc7(p)*Lc);

% Finite difference equation--explicit method.
H4(p)=(delt/(rho7(p)*cp7(p)*V4));
T7(p+1)=2*(((H4(p)/Rt3(p))*(T6(p)-T7(p)))+((H4(p)/Rc4(p))*(T8(p)-T7(p)))+((T7(p)+
T8(p))/2))-T8(p);

T8(p+1)=2*(((H4(p)/Rc4(p))*(T7(p)-T8(p)))+((T7(p)+T8(p))/2))-T7(p+1);

if T8(p+1)<300
T8(p+1)=300;
else
T8(p+1)=T8(p+1);
end
end
t=t/60;

plot(t,T8); grid;
xlabel('Time (min)');
ylabel('Temperature (K)');
```

# APPENDIX D. TIME-TEMP PROFILE AT EACH NODE

The following figures show the time-temperature profile for each node in the resistance network. These four figures reflect Scenario 1. Figures 24 and 25 reflect the CCL-FIRE program code which solves for surface radiative resistance explicitly. Figures 26 and 27 reflect the CCL-FIRE program code which solves for the surface radiative resistance with a Taylor series expansion.

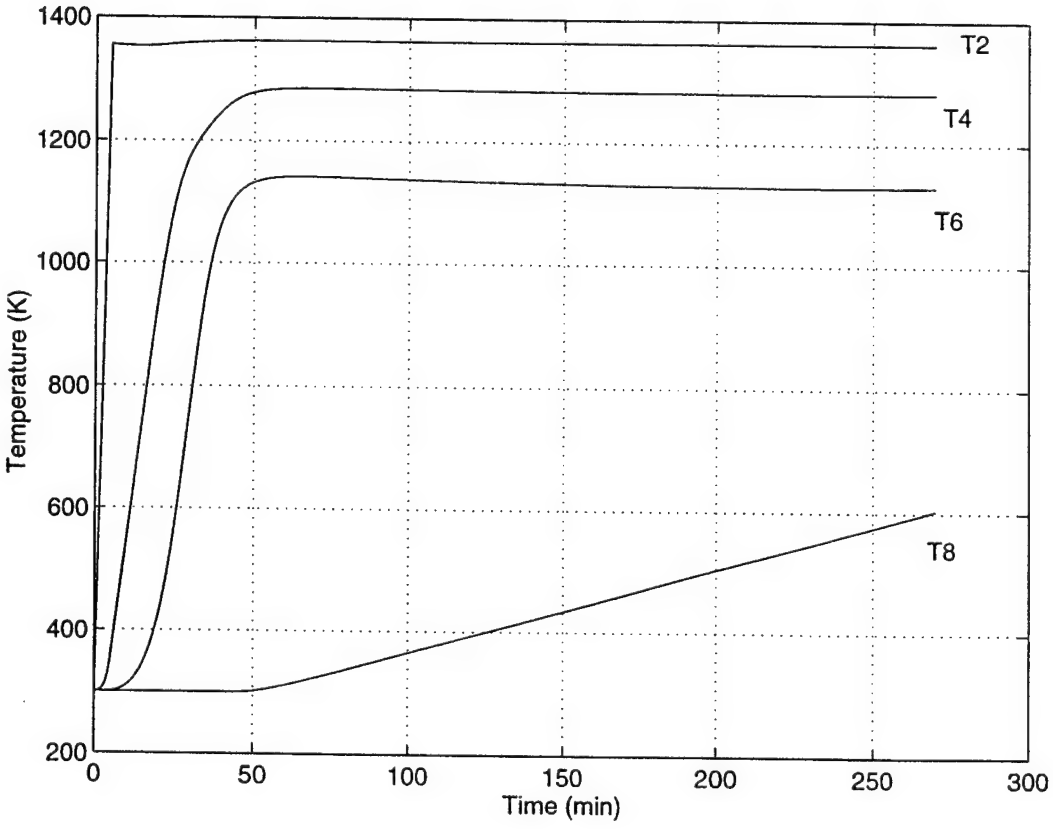


Figure 24. Scenario 1A - Node Time-Temperature Profiles.

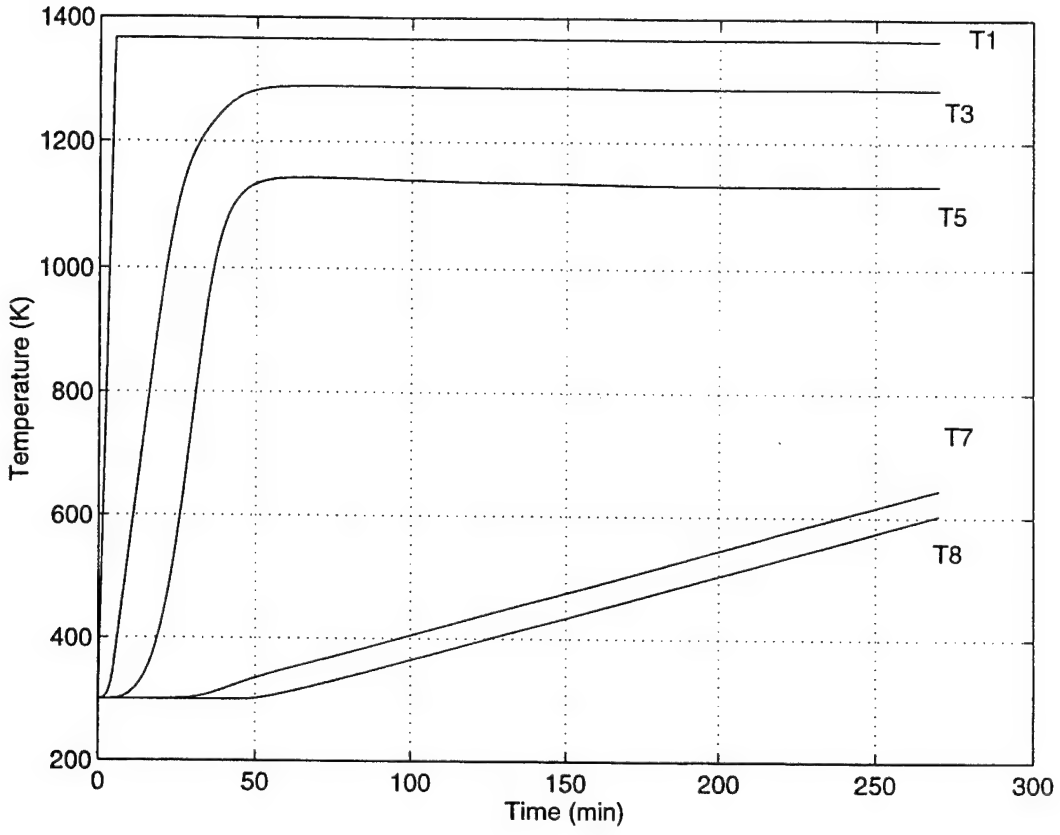


Figure 25. Scenario 1A - Node Time-Temperature Profiles.

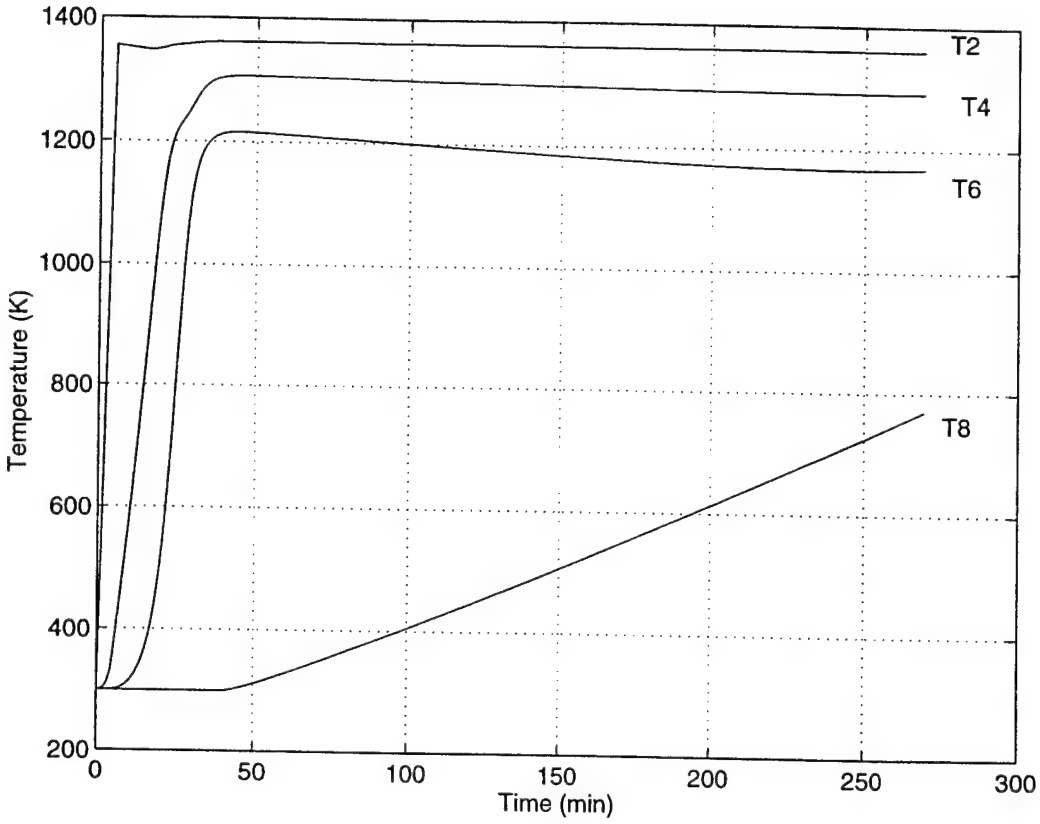


Figure 26. Scenario 1B - Node Time-Temperature Profiles.

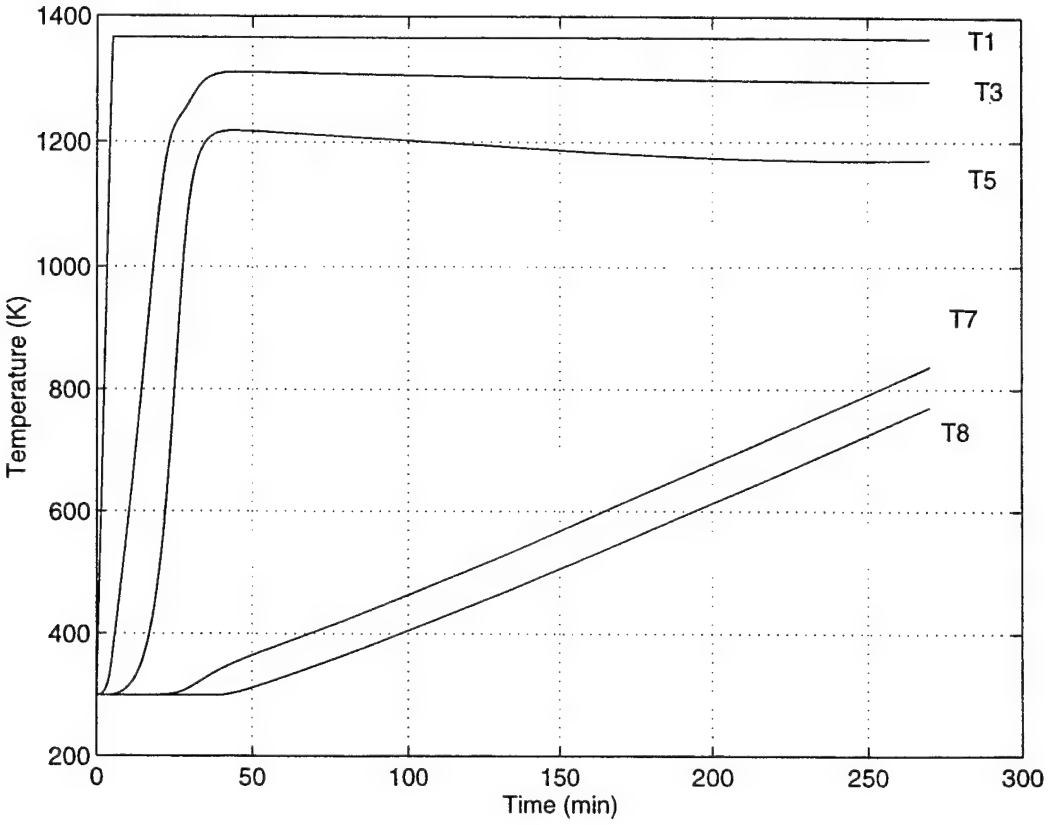


Figure 27. Scenario 1B - Node Time-Temperature Profiles.

# LIST OF REFERENCES


1. Bowman, H.L. and Lee, M.J. *Magazine Fire Protection: An Assessment of Magazine Vulnerability to Fire*, Research and Technology Division, Naval Air Warfare Center Weapons Division, Mar 95.

2. Barker, T., Maillie, F., Burton, T., Rudnicki, R., and Frick, J. *Concentric Canister Launcher Concept Evaluation Report*, Dahlgren Division, Naval Surface Warfare Center, Oct 94.

3. Mansfield, J. A. *Preliminary Analysis of the Heating of Ordinance in Ship Magazines Due to a Fire in an Adjacent Compartment*, Airframe, Ordnance, and Propulsion Division, Naval Air Warfare Center Weapons Division, Sep 96.

4. Incropera, F.P. and DeWitt, D.P., *Introduction to Heat Transfer*, John Wiley & Sons, Inc., 1990.

5. Gebhart, B., Jaluria, Y., Mahajan, R. L., and Sammakia, B., *Buoyancy-Induced Flows and Transport*, Hemisphere Publishing Corp., 1988.

6. Touloukian, Y. S., and Ho C. Y., Eds., *Thermophysical Properties of Matter*, Plenum Press, New York; Vol. 1, *Thermal Conductivity of Metallic Solids*; Vol. 4, *Specific Heat of Metallic Solids*; Vol. 7, *Thermal Radiative Properties of Nonmetallic Solids*; 1972.

7. Churchill, S. W., "Free Convection in Layers and Enclosures," *Heat Exchanger Design Handbook*, Vol. 2, Hemisphere Publishing Corp., 1983.

8. The Math Works, Inc., *The Student edition of MATLAB*, Prentice-Hall, Inc., 1995.

9. Howell, J. R., *A Catalog of Radiation Configuration Factors*, McGraw-Hill, Inc., 1982.

10. Modest, M. F., *Radiative Heat Transfer*, McGraw-Hill, Inc., 1993.

11. Conversation Between Les Bowman, NAWC - Weapons Division, and LT Tim Callaham, Naval Postgraduate School - Dept. of Mechanical Engineering, of November 1996.

# INITIAL DISTRIBUTION LIST

1. Defense Technical Information Center . . . . . 2
   8725 John J. Kingman Road, Ste 0944
   Ft. Belvoir, Virginia 22060-6218

2. Dudley Knox Library . . . . . 2
   Naval Postgraduate School
   411 Dyer Road
   Monterey, California 93943-5101

3. Naval/Mechanical Engineering Curricular Officer, Code 34 . . . . . 1
   Naval Postgraduate School
   Monterey, California 93943-5101

4. Professor Matthew D. Kelleher . . . . . 3
   Mechanical Engineering Department, Code ME/KK
   Naval Postgraduate School
   Monterey, California 93943-5101

5. LT Timothy P. Callaham, USN . . . . . 3
   227 San Bernabe Drive
   Monterey, California 93940

6. LT Gary Null, USN . . . . . 1
   1247 Spruance Road
   Monterey, California 93940

7. Commander, NSWCDD . . . . . 1
   Attn: J. Yagla, G70
   Dahlgren, Virginia 22448

8. NAWC-Weapons Division . . . . . 1
   Fire Research Office Code: 4B3100D
   Attn: L. Bowman
   China Lake, California 93555-6100

9. NAWC-Weapons Division . . . . . 1
   Fire Research Office Code: 4B3100D
   Attn: J. Hoover
   China Lake, California 93555-6100

10. Naval Sea Systems Command . . . . . 1
Attn: Brian Smale
NAVSEA 03R12
2531 Jefferson Davis Hwy
Arlington, Virginia 22242-5160